

Cite this: *Chem. Sci.*, 2025, **16**, 2062

All publication charges for this article have been paid for by the Royal Society of Chemistry

Received 15th October 2024  
Accepted 8th January 2025

DOI: 10.1039/d4sc07009g  
rsc.li/chemical-science

## Introduction

N-Heterocyclic carbenes (NHCs) represent one of the most significant and extensively studied families of ligands in organometallic chemistry. Their robust  $\sigma$ -donating properties and ability to stabilize transition metals have made them indispensable in the chemistry of Late Transition Metals (LTM), where they have been widely employed as supporting ligands in a plethora of catalytic processes. Over the past few decades, the utility of NHCs has expanded far beyond traditional metal catalysis, finding applications in a range of fields such as in organocatalysis.<sup>1,2</sup> Moreover, NHCs have been effectively incorporated into f-block metal chemistry,<sup>3</sup> materials science,<sup>4</sup> and surface chemistry,<sup>5</sup> demonstrating their versatility and adaptability. These ligands have also been explored in biomedical research in the development of therapeutic agents,<sup>6</sup> as well as in Main group chemistry,<sup>7</sup> further illustrating their broad applicability across diverse areas of chemical research space.

The rapid development and research into N-heterocyclic carbenes occurred shortly after Bertrand's isolation of the first stable  $\lambda^3$ -phosphinocarbene (1989)<sup>8</sup> and Arduengo in 1991, who isolated the first stable NHC – IAd (1,3-di(adamantyl)imidazole-2-ylidene).<sup>9</sup> These breakthroughs built upon seminal work of Wanzlick and Öfele (dating back to 1968) who independently synthesized the first NHC complexes with mercury and chromium.<sup>10,11</sup> The field saw further advances in 1995 with Herrmann's seminal report, showing the utility of NHC ligands in palladium-catalyzed Heck cross-coupling reactions.<sup>12</sup> This reporting is a key moment where transition metal–NHC complexes were shown to have catalytic relevance.

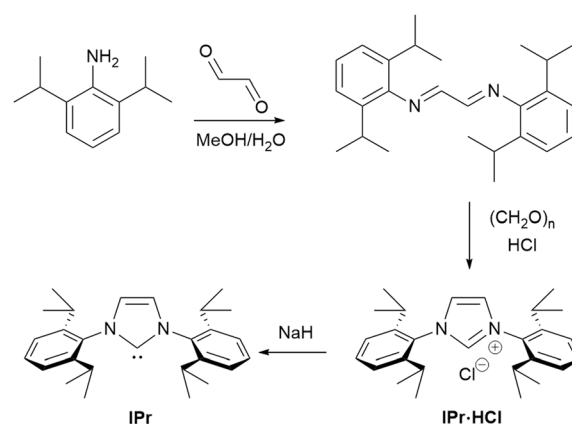
The IPr ligand was first introduced by the Nolan group in 1999.<sup>13,14</sup> The modified synthetic method is based on an

## The influential IPr: 25 years after its discovery

Vladislav A. Voloshkin, Leandros P. Zorba and Steven P. Nolan \*<sup>\*</sup>

N-Heterocyclic carbenes (NHCs) have emerged as a privileged ligand family in organometallic chemistry, widely recognized for their unique steric and electronic properties. Among them, the 1,3-bis(2,6-diisopropylphenyl)imidazole-2-ylidene (IPr) ligand has become a cornerstone of NHC chemistry for its remarkable versatility, stability, and broad use. Since its discovery by the Nolan group in 1999, IPr has played a pivotal role in advancing catalytic transformations and facilitating the utilization of NHC ligands in various domains. This article highlights major contributions where IPr has helped shape modern organometallic chemistry, with a focus on its influence in transition metal catalysis and ligand design. Twenty five years after its discovery, the IPr ligand continues to be a benchmark ligand, inspiring and driving innovation.

important adaptation of the general protocol reported by Arduengo.<sup>15</sup> This straightforward two-step process (Scheme 1) begins with the use of the readily available 1,3-diisopropylbenzene to form a diimine, which, after simple collection as a solid *via* filtration, can be subjected to cyclization using para-formaldehyde. The imidazolium salt is formed with an accompanying counterion, which originates from the protic acid or TMSCl used. Following another filtration, the resulting bench-stable and easy-to-handle precursor can be immediately used either for the generation of the free carbene or for the direct synthesis of metal complexes. The simplicity of this method, which eliminates the need for rigorous purification steps, combined with the robustness and stability of the precursors, has further enhanced the appeal and widespread use of the IPr ligand in catalysis. Its practicality and stability have made it a highly attractive first choice for researchers in organometallic chemistry.



Scheme 1 Synthesis of IPr·HCl and IPr.





Fig. 1 High- and low-tech reactors for the synthesis of  $\text{IPr}\cdot\text{HCl}$ .

The synthetic protocol of the imidazolium salt ( $\text{IPr}\cdot\text{HCl}$ ) has proven quite robust and has been conducted in the Nolan labs on two continents and in 5 countries using high volume glass reactors and in a low-tech apparatus (Fig. 1). The detailed protocol for large scale synthesis of imidazolium salt and free carbene has been disclosed by the Nolan group.<sup>16</sup> The free NHC **IPr** (1,3-bis(2,6-diisopropylphenyl)imidazole-2-ylidene) holds a unique and distinguished position among NHC ligands, despite not being the first NHC to be isolated or employed in catalysis. As it turns out, it is often the ligand of choice in any new catalyst screening involving an NHC. Its significance lies in its remarkable versatility, stability and broad applicability, making it one of the most widely used and influential ligands within the entire NHC family. The success of **IPr** can not only be attributed to its utility as a supporting ligand but also as inspiration in the development of related ligands. These evolutions in ligand design, oftentimes built around the **IPr** core, have permitted great advances in reactivity and catalysis.

Since its discovery, **IPr** has emerged as a cornerstone of NHC-based chemistry, featuring prominently in over 1800 scientific publications covering various domains of chemical science. However, the bibliographical metrics are somewhat misleading as the ligand and complexes are nowadays so commonly used that the primary literature goes often uncited. As one of the most readily accessible, its utilization as an ancillary ligand has often streamlined research efforts, causing a substantial increase in the exploration and application of NHCs in catalysis.

This account provides an overview of seminal contributions enabled using the **IPr** ligand, with particular focus on the pioneering advances that catalyzed the exploration of NHC as supporting ligands. While many examples of **IPr**-metal complexes have been reported, encompassing not only early and late transition metals<sup>17–20</sup> but also Main group, and f-block elements,<sup>3,7</sup> this contribution will focus on specific metals where **IPr** has had the greatest influence on their chemistry and catalytic applications. Additionally, we will examine the far-reaching influence of the **IPr** framework on ligand design and methodology development over the 25 years since its discovery, emphasizing its role in shaping modern organometallic chemistry.

## Ruthenium chemistry and **IPr**

The first article employing **IPr** was devoted to the use of  $[\text{Ru}(\text{p}-\text{cymene})(\text{NHC})\text{Cl}_2]$  complexes in ring-closing metathesis (RCM).<sup>21</sup> Olefin metathesis plays a pivotal role in modern

chemistry, as evidenced by the Nobel Prize in Chemistry in 2005 awarded for the development of this transformative method in organic synthesis. Interestingly, the research groups of Nolan,<sup>22</sup> Grubbs,<sup>23</sup> and Herrmann/Fürstner<sup>24</sup> independently reported on mono-NHC-based ruthenium catalysts for olefin metathesis in the same year as when the **IPr** ligand was introduced. These catalysts, bearing IMes (1,3-bis(2,4,6-trimethylphenyl)imidazole-2-ylidene) and SIMes (1,3-bis(2,4,6-trimethylphenyl)imidazolin-2-ylidene), mostly, are now known as second-generation Grubbs' catalysts.

Catalytic activities of *p*-cymene **IPr** complex **Ru-1** (Fig. 2) together with the IMes congener were tested in RCM employing diethyldiallylmalonate.<sup>21</sup> Both IMes and **IPr** complexes showed high efficiency as catalyst precursors, with IMes being more active at 40 °C, achieving higher conversions than **IPr** under these conditions (Scheme 2a). However, at elevated temperatures (80 °C), both complexes exhibited similar catalytic activities, indicating that temperature played a key role in overcoming activation barriers in this transformation and using these two distinct NHCs. This study also highlighted the superior stability of these NHC ligands compared to phosphine-based systems, demonstrating their robustness at elevated temperatures.

Subsequently, similar studies were performed with other precatalysts incorporating the alkylidene, 3-phenyldienylidene.<sup>25</sup> Notably, while the IMes complex was more efficient in reactions involving diethyldiallylmalonate, the **IPr** complex **Ru-2** outperformed IMes in reactions with diallyltosylamine (Scheme 2b). Stability tests further confirmed that both IMes and **IPr** complexes remain stable at 80 °C for over 10 days without any sign of decomposition, highlighting their robustness under prolonged thermal conditions. The advantageous

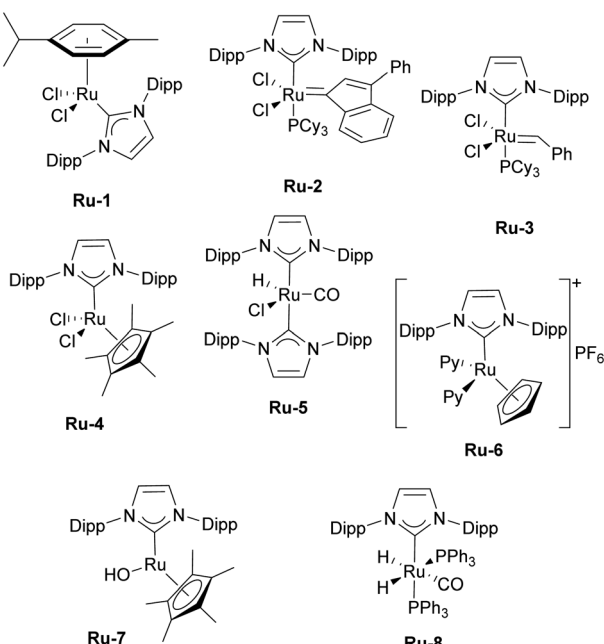
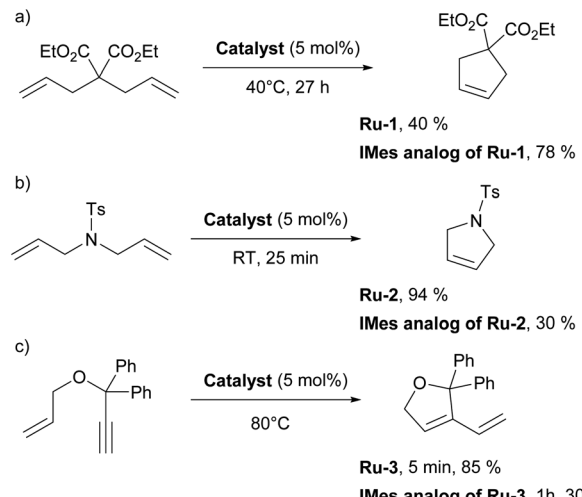


Fig. 2 Selected examples of **IPr**-ruthenium complexes. Dipp = 2,5-diisopropylphenyl, Py = pyridine.



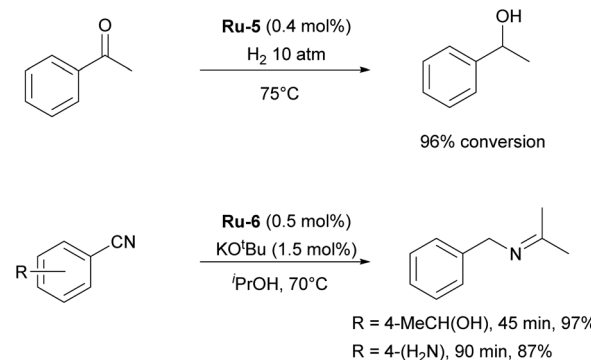
**Scheme 2** Examples of the use of **Ru-1** (a), **Ru-2** (b) and **Ru-3** (c) in Ring Closing Metathesis (RCM).

role of the **IPr** ligand had yet to be fully demonstrated in olefin metathesis, but this was to come shortly (*vide infra*).

Subsequently, several comparative studies including **IPr** ruthenium complexes were reported. Fürstner showed that **IPr**-ruthenium complex **Ru-3** (Fig. 2) in some cases outperformed **IMes** congeners and had as fast initiation rate for enyne metathesis as the state-of-the-art at a time, the **IMes** analog (Scheme 2c).<sup>26</sup> The nature of the increased catalytic activity between first and second generation ruthenium olefin metathesis catalysts was studied on the example of **IPr**, revealing that it slowed bimolecular carbene decomposition in the 14-electron ruthenium intermediate during catalysis,<sup>27</sup> thus leading to significantly increased activity and thermal stability (because of the increased steric bulk of **IPr**) compared to first generation catalysts. In another study,  $[\text{Ru}(\text{Cp}^*)(\text{IPr})\text{Cl}]$  complex **Ru-4** was studied to explain the difference in catalytic activity between saturated and unsaturated NHCs in ruthenium catalyzed olefin metathesis (Fig. 2), revealing that even slight differences in electronic and steric properties of the NHC could cause drastic differences in catalytic activity.<sup>28</sup>

Even though **IMes** and especially **IMes** ruthenium complexes became go-to catalysts in olefin metathesis, those highly cited important studies, featuring the **IPr** ligand, contributed to the increased interest and subsequent improved understanding and popularity of the NHC-containing ruthenium metathesis catalysts. The **Ru-IPr** based systems proved to be excellent olefin metathesis systems but are less frequently employed, we feel, because the **IMes**-based system had, by then, taken a strong hold on the market.

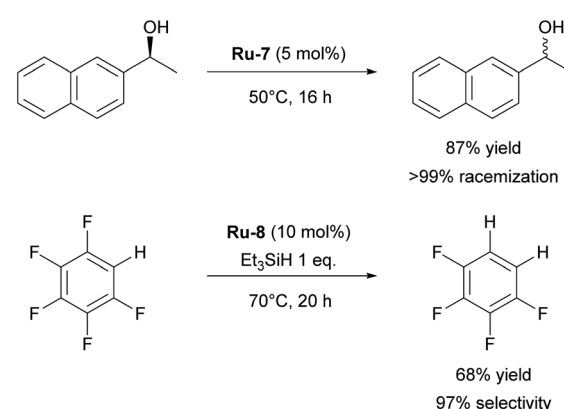
Although highly impactful, the **IPr**-ruthenium chemistry is not only limited to olefin metathesis. Another field where **IPr**-ruthenium complexes were implemented is in hydrogenation reactions. One of the first examples of the use of **IPr**-Ru complex in hydrogenation was reported by the Whittlesey group<sup>29</sup> who showed that among a series of  $[\text{Ru}(\text{NHC})(\text{L})(\text{CO})(\text{H})\text{Cl}]$  complexes, the most efficient catalyst for the hydrogenation



**Scheme 3** Examples of the use of **Ru-5** and **Ru-6** in hydrogenation reactions.

of acetophenone (Scheme 3) was the **IPr**-based **Ru-5** (Fig. 2). Later on, the Nikonov group reported efficient transfer hydrogenation of nitriles and olefins, catalyzed by half-sandwich ruthenium complexes incorporating **IPr** as ancillary ligand, with best results obtained using **Ru-6** (Fig. 2 and Scheme 3).<sup>30</sup> The developed protocol allowed for the hydrogenation of nitriles, activated heterocycles such as quinoline, and various olefins. It was shown that these catalysts perform better than phosphine-based cousins.

Another interesting example of the use of **IPr** as a ligand is its role as a stabilizing ligand for the isolation of reactive species. It has been shown that heterobimetallic catalyst (**IMes**)  $\text{AgRuCp}(\text{CO})_2$  is a highly efficient and selective catalyst for *E*-selective semi-hydrogenation of alkynes.<sup>31</sup> However, attempts to isolate intermediates with **IMes** as ancillary ligand in order to study the mechanism failed. Therefore, authors turned to **IPr** analogs of those intermediates and managed their isolation and proposed a mechanism for the transformation. This is also a recurring theme encountered in Transition Metal (TM) **IPr** chemistry: the improved crystallinity/stability of the **IPr**-derived complexes. NHC-ruthenium complexes have also been employed in the racemization of chiral alcohols. Although **ICy**-based complex proved to be more efficient than the **IPr** counterpart, in the presence of strong base,<sup>32</sup> ruthenium hydroxide



**Scheme 4** Examples of the use of **Ru-7** and **Ru-8** in racemization of alcohols and hydrodefluorination, respectively.



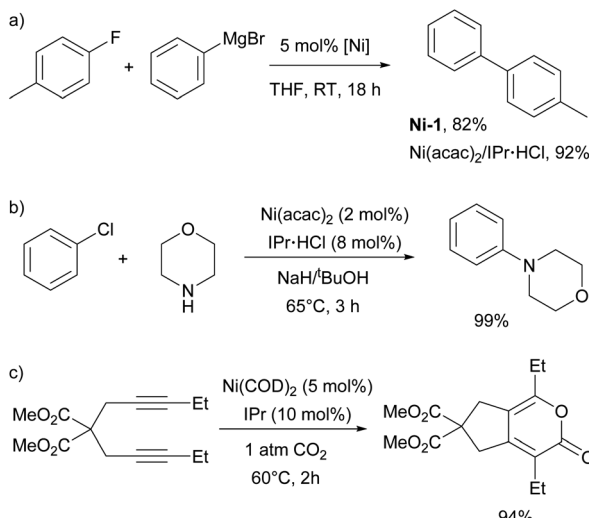
complex **Ru-7** (Fig. 2) bearing **IPr** could catalyze this transformation for secondary alcohols without base (Scheme 4).<sup>33</sup>

The Whittlesey group has reported on the catalytic hydrodefluorination of aromatic fluorocarbons using  $[\text{Ru}(\text{NHC})(\text{PPh}_3)_2(\text{CO})\text{H}_2]$  complexes. During their studies, the **IPr**-based catalyst **Ru-8** (Fig. 2) showed the highest catalytic activity in hydrodefluorination of pentafluorobenzene in the presence of  $\text{Et}_3\text{SiH}$  (Scheme 4).<sup>34</sup> The follow-up mechanistic study of this reaction revealed the effects behind the unusual selectivity of this process which turned out to be dependent on the nature and properties of the NHC ligand.<sup>35</sup>

In summary, the **IPr** ligand has played a pivotal role in advancing ruthenium chemistry, particularly in the fields of olefin metathesis and hydrogenation. These contributions have not only improved reaction efficiency and selectivity, but also broadened the scope of ruthenium-catalyzed transformations, solidifying the importance of **IPr** in established areas of ruthenium catalysis.

### Nickel catalysis and **IPr**

The first report on the **IPr**-nickel complexes dates back to 2001, when Hermann used  $\text{IPr}_2\text{Ni}(0)$  complex **Ni-1** (Fig. 3) for room temperature Kumada–Tamao–Corriu coupling between aryl fluorides and aryl Grignard reagents.<sup>36</sup> Interestingly, *in situ* generated catalyst from  $[\text{Ni}(\text{acac})_2]$  and imidazolium salt proved to be slightly more efficient than well-defined complex (Scheme 5a). This was attributed to the fact that mono-ligated **IPr**-Ni(0) was the active species in this transformation and a species bearing two such units would necessitate a ligand displacement to form the active species. Simultaneously, the Fort group reported the use of the  $[\text{Ni}(\text{acac})_2]/\text{IPr}\cdot\text{HCl}$  catalytic system for amination of aryl chlorides (Scheme 5b).<sup>37</sup> Louie *et al.* also reported on the use of *in situ* generated **IPr**-Ni catalyst for



Scheme 5 Early examples of the use of **IPr** ligand in Ni catalysis.

the  $[2 + 2 + 2]$  cycloaddition of  $\text{CO}_2$  and diynes (Scheme 5c).<sup>38</sup> A year later, Dible and Sigman reported the isolation of the first mono-ligated Ni(II) complex **Ni-2** with **IPr** as ancillary ligand (Fig. 3).<sup>39</sup>

Another highly influential study, not only for Ni–NHC chemistry, but one affecting the broader field of NHCs, was conducted by Nolan in the elucidation and quantification of the steric and electronic properties of NHCs. The synthesis and characterisation *via* IR spectroscopy of  $[\text{Ni}(\text{CO})_3(\text{NHC})]$  complexes were used to measure the CO stretching frequencies leading to determination of Tolman electronic parameter (TEP).<sup>40</sup> At the same time, the results from diffraction studies on single crystals were used to calculate the percent buried volume ( $\%V_{\text{bur}}$ ) of the NHC ligands, providing valuable insights into their steric properties.<sup>41</sup> This work became the basis for further studies and development of steric descriptors for NHCs which are widely used in explaining the catalytic activity of NHC metal complexes.<sup>42–46</sup>

These pioneering studies have permitted significant advances in the development of NHC–Ni chemistry. Unlike in ruthenium chemistry, where IMes-based catalysts dominate, **IPr** remains one of the most widely used monodentate NHC ligands in nickel chemistry and catalysis. The incorporation of NHC ligands not only enabled milder reaction conditions and enhanced selectivity but also facilitated new catalytic transformations. Among the most explored reactions in this area are cross-couplings—particularly Suzuki–Miyaura, Kumada–Tamao–Corriu, and Buchwald–Hartwig reactions—along with  $\alpha$ -arylation, C–H functionalization, reductive couplings, cycloadditions, and hydrosilylation, although this short listing is by no means exhaustive.

Building on the Hermann work, several subsequent studies explored Kumada–Tamao–Corriu (KTC) couplings with **IPr**-Ni complexes, with two particularly influential examples being the use of **Ni-2** and the dinuclear Ni(II)–**IPr** complex, **Ni-3** (Fig. 3). In the first study, the authors successfully performed KTC

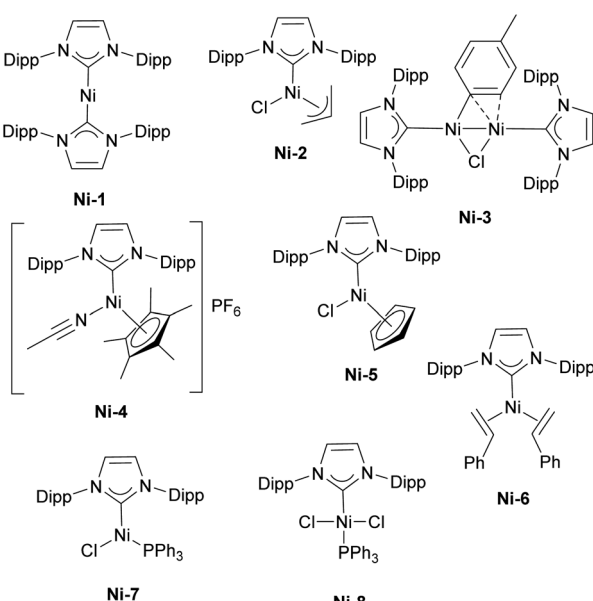


Fig. 3 Selected examples of the **IPr**-nickel complexes used in catalysis.

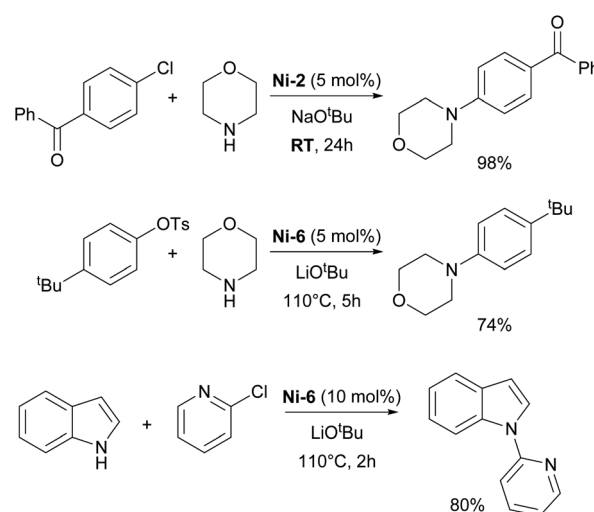


coupling reactions with both heteroaromatic chlorides and anisoles under relatively mild conditions.<sup>47</sup> The second study provided crucial insights into the catalytic cycle, specifically highlighting the involvement of dinuclear monovalent nickel complexes in the reaction mechanism. These findings have greatly improved the understanding of Ni-catalyzed cross-coupling reactions and the role of **IPr** in enhancing their efficiency.<sup>48</sup>

Regarding the Suzuki–Miyaura coupling, polydentate NHC nickel complexes have dominated the field. However, it should be mentioned that in a comparative study of half-sandwich NHC–nickel(II) complexes, the **IPr** complex **Ni-4** (Fig. 3) showed the best reaction rate in the Suzuki–Miyaura coupling (Scheme 6).<sup>49</sup> Another Ni–**IPr** complex **Ni-5** (Fig. 3) recently showed high catalytic activity in Suzuki–Miyaura coupling of amides under aerobic conditions.<sup>50</sup>

Following Fort's work, several studies have appeared on the use of Ni–NHC catalytic systems for amination reactions. In 2005, Schneider introduced the *in situ* generation of the **Ni-1** complex for efficient amination of aryl chlorides, demonstrating that **IPr** provided superior reactivity compared to other ligands.<sup>51</sup>

The Nicasio group utilized the previously mentioned allyl complex, **Ni-2**, for the amination of (hetero)aryl chlorides under mild conditions, showcasing, for the first time, that this transformation could be achieved at room temperature with a nickel pre-catalyst (the IMes-coordinated congener of **Ni-2** exhibited very poor reactivity).<sup>52</sup> Building on this work, the same group developed another pre-catalyst,  $[\text{Ni}(\text{IPr})(\text{styrene})_2]$  (**Ni-6**, Fig. 3), which was successfully applied to the amination of aryl tosylates,<sup>53</sup> and later to the *N*-arylation of indoles and carbazoles (Scheme 7).<sup>54</sup> Another important report featuring **IPr** was

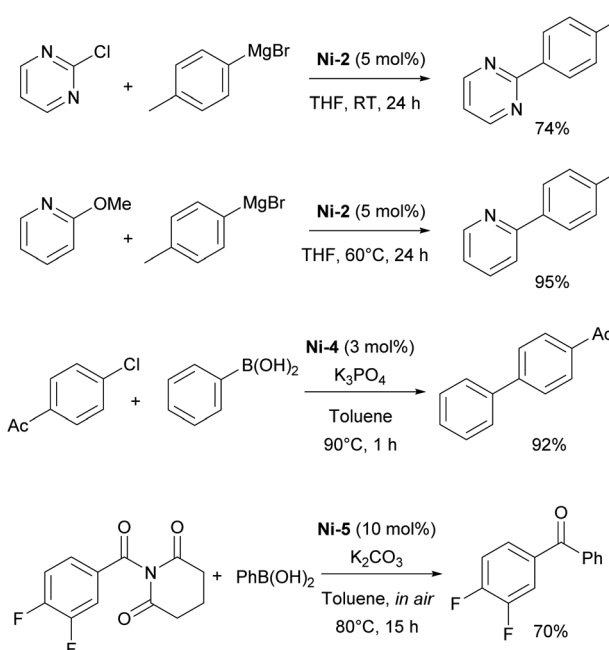


Scheme 7 IPr–nickel complexes in amination reactions.

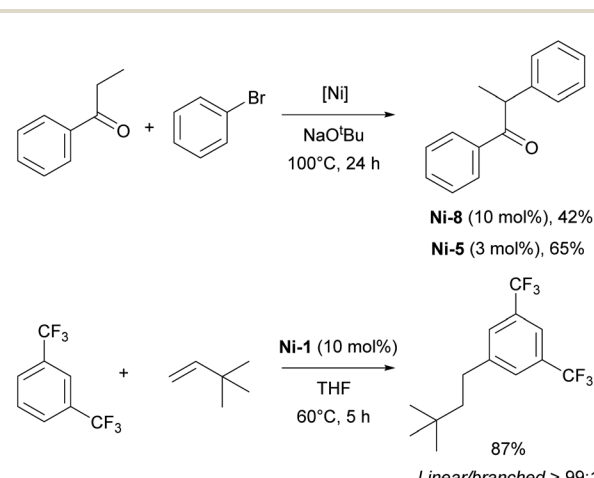
devoted to the use of Y-shaped monovalent nickel complex **Ni-7** (Fig. 3), which enabled the amination of arylhalides with diphenylamine at room temperature, an unprecedented result, at the time.<sup>55</sup> One of the latest examples where **IPr** ligand was used to stabilize active intermediates in nickel catalysis is the mechanistic study of the Ni(I)–Ni(III) catalytic cycle in the Buchwald–Hartwig amination.<sup>56</sup>

In 2014, Hartwig and co-workers reported the hydroarylation of olefins with trifluoromethyl-substituted arenes using the  $[\text{Ni}(\text{IPr})_2]$  **Ni-1** complex. This transformation displayed unprecedented selectivity for the linear *anti*-Markovnikov product.<sup>57</sup>

The  $\alpha$ -arylation transformation is another reaction where **IPr**–Ni complexes have been successfully employed. Matsubara *et al.* utilized a mixed NHC/PR<sub>3</sub> nickel complex containing **IPr** (**Ni-8**, Fig. 3) for the arylation of propiophenones with various aryl halides, although this required a relatively high catalyst loading of 10 mol% at an elevated temperature of 110 °C (Scheme 8).<sup>58</sup> Several years later, the Ritleng group reported the



Scheme 6 IPr–nickel complexes in KTC and Suzuki–Miyaura couplings.



Scheme 8 IPr–nickel complexes in  $\alpha$ -arylation and hydroarylation reactions.

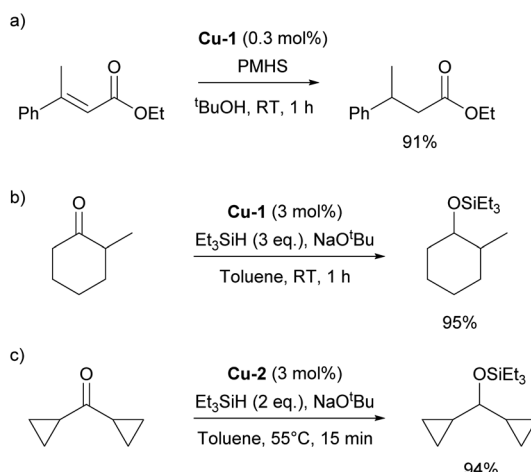


use of the half-sandwich complex **Ni-5**, which permitted to reduce the catalyst loading to 3 mol% and to broaden the reaction scope (the IMes-congener of **Ni-5** was not very efficient, leading to a 25% yield, using 5 mol% catalyst loading, whereas **Ni-5** afforded a 78% yield with 3 mol% catalyst loading).<sup>59</sup> Further advances were made by increasing the steric bulk of the **IPr** core structure with phenyl substituents, leading to improved efficiency in the  $\alpha$ -arylation reaction.<sup>60</sup> This ground-breaking work laid the foundation for a series of studies in which either **IPr** or modified **IPr**-based ligands were employed to further enhance selectivity and expand the reaction scope to include very challenging substrates.<sup>61–63</sup>

Additionally, it is important to highlight other key contributions to NHC–nickel chemistry, where the **IPr** ligand has played a pioneering role in facilitating the development of novel methods and reactions. These include (but are not limited to) the use of **IPr**–Ni complexes in hydrosilylation,<sup>64,65</sup> C–H functionalization polycondensation,<sup>66</sup> dual photoredox catalysis<sup>67</sup> and metalloradical catalysis.<sup>68,69</sup>

### Copper catalysis and **IPr**

The history of NHC–copper chemistry began in 1993 when Arduengo reported the synthesis of the first homoleptic NHC complexes of copper.<sup>70</sup> Since then, numerous reports featuring NHC–copper complexes in organometallic chemistry and their deployment in catalysis have been published. A significant milestone came with the work of Buchwald and co-workers, who synthesized the first well-defined **IPr**-containing copper complex, **Cu-1** (Fig. 4), which played a pivotal role in advancing this field. This complex proved to be highly efficient in the conjugate reduction of  $\alpha,\beta$ -unsaturated carbonyl compounds, setting a new standard for catalytic performance at the time



Scheme 9 Use of **Cu-1** (a and b) and **Cu-2** (c) in conjugate reduction and hydrosilylation of ketones.

(Scheme 9a).<sup>71</sup> The reaction mechanism was proposed to involve the formation of an NHC–copper hydride intermediate, generated through the reaction of *in situ* formed  $[\text{Cu}(\text{NHC})(\text{O}^{\prime}\text{Bu})]$  and polymethylhexasilazane (PMHS), a hypothesis later confirmed by stoichiometric experiments conducted by Sadighi.<sup>72</sup> NHC ligands played a pivotal role in the use of copper complexes in catalysis in general, with **IPr** being often the first NHC ligand successfully employed in the development of a new transformation or improvement of existing ones.

In the same year as Buchwald reported the synthesis of the first **IPr**–copper complex, Nolan and co-workers utilized this catalytic system in the hydrosilylation of ketones at room temperature (Scheme 9b).<sup>73</sup> In the follow-up study, the Nolan group introduced cationic complex **Cu-2** (Fig. 4) to mediate the same transformation, which proved to be slightly more efficient and allowed for an expanded reaction scope (Scheme 9c).<sup>74</sup> A slightly different reaction mechanism was proposed for the cationic complex, where dissociation of one of the **IPr** ligands occurs prior to formation of the *tert*-butoxide intermediate.<sup>75</sup>

Other important contributions opening the way for various catalytic transformations mediated by NHC–copper complexes came from Sadighi and Petersen on insertions into Cu–alkyl bond. The insertion of  $\text{CO}_2$  into  $\text{Cu}-\text{CH}_3$  under mild conditions to form copper acetate was established in the first report.<sup>76</sup> This reactivity, along with Sadighi's earlier findings on the interaction of copper alkoxide species with B–B bonds,<sup>77</sup> paved the way for Hou's important development of the carboxylation of organoboronic esters, catalyzed by  $[\text{Cu}(\text{IPr})\text{Cl}]$  (Scheme 10).<sup>78</sup> The Hou research group also reported on the hydrosilylation of carbon dioxide using  $[\text{Cu}(\text{IPr})(\text{O}^{\prime}\text{Bu})]$  (**Cu-3**, Fig. 4) as the catalyst, further expanding the scope of copper-mediated transformations to  $\text{CO}_2$  activation/conversion (99% vs. 74% yield for the hydrosilylation of carbon dioxide, between **Cu-3** and the corresponding IMes-coordinated congener, at 100 °C).<sup>79</sup>

Further studies revealed that the  $[\text{Cu}(\text{IPr})(\text{CH}_3)]$  complex reacts with various compounds containing acidic N–H, C–H, and O–H bonds, leading to the formation of  $[\text{Cu}(\text{IPr})\text{X}]$  species

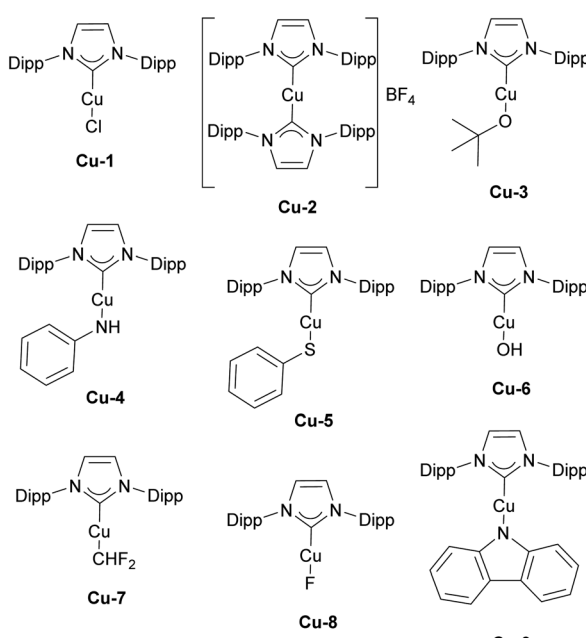
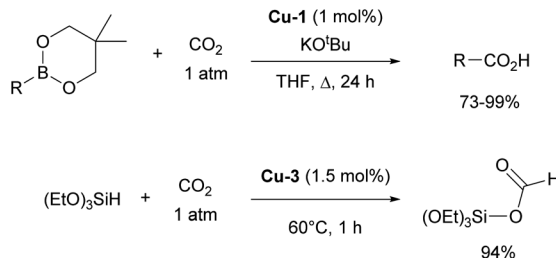


Fig. 4 A selection of **IPr**–copper complexes used in catalysis.

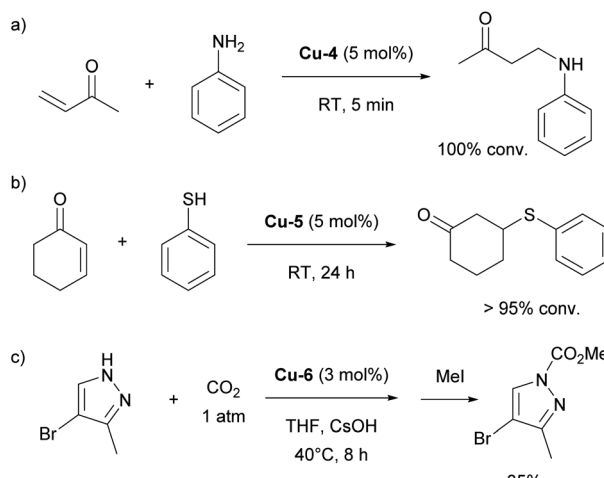


Scheme 10 IPr–Cu complexes in  $\text{CO}_2$  insertion chemistry.

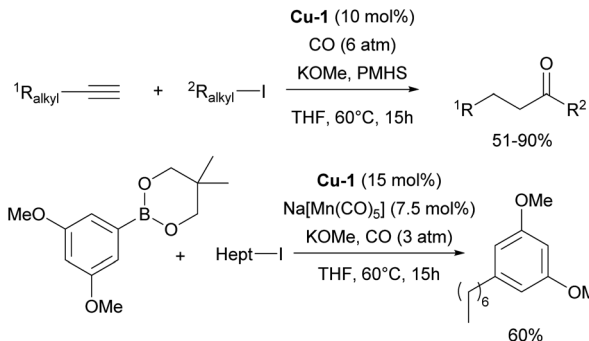
and the release of methane.<sup>80,81</sup> These  $[\text{Cu}(\text{IPr})\text{X}]$  complexes were subsequently employed as catalysts for *anti*-Markovnikov additions of N–H and O–H bonds to olefins (Scheme 11a).<sup>82</sup> The same strategy was extended to the hydrothiolation of olefins using  $[\text{Cu}(\text{IPr})(\text{SR})]$  catalysts (Scheme 11b).<sup>83</sup>

In 2010, the Nolan group introduced a new IPr–copper hydroxide complex, Cu-6 (Fig. 4), which possessed the ability to activate various C–H bonds under mild conditions.<sup>84</sup> This property allowed for the *in situ* formation of  $[\text{Cu}(\text{IPr})\text{R}]$  species containing Cu–C bonds, which were later used successfully in the catalytic carboxylation of C–H and N–H bonds (Cu-6 exhibited higher reactivity than the SIPr-, IMes- and SIMes-coordinated congeners, 69% vs. 28% vs. 16% vs. 23%, using 2-methyl-1*H*-imidazole as reagent and 1 mol% catalyst loading, respectively), utilizing  $\text{CO}_2$  as a reagent (Scheme 11c).<sup>85</sup>

Recently, numerous reports have focused on the use of NHC–copper complexes, particularly IPr–Cu complexes, in carbonylative and borylative transformations. The Mankad group has reported on hydrocarbonylative couplings of alkynes with alkyl halides, where the  $[\text{Cu}(\text{IPr})\text{Cl}]$  complex proved to be the most efficient for coupling alkyl iodides with both terminal and internal alkynes (Scheme 12).<sup>86,87</sup> Following these reports, a carbonylative C–C coupling of arylboronic esters with alkyl halides for the synthesis of ketones was developed, using a dual Mn/Cu catalytic system. This method is compatible with various



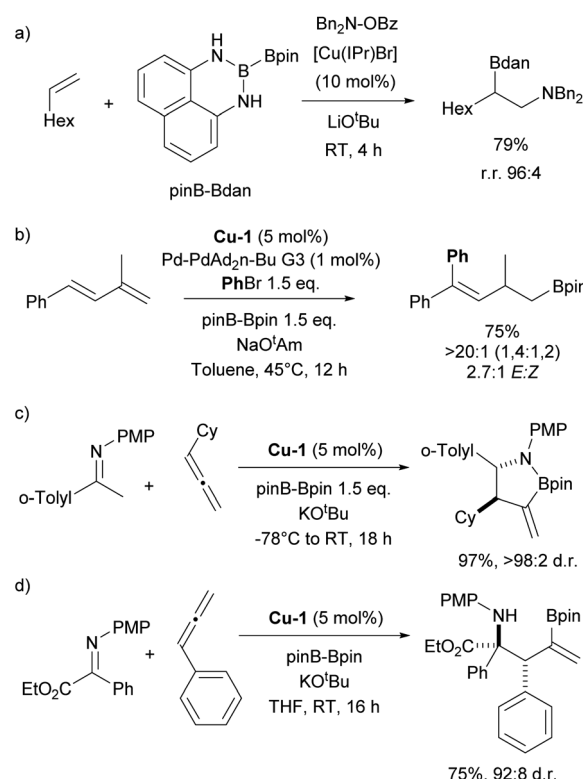
Scheme 11 Use of IPr–Cu in hydroamination, hydrothiolation and carboxylation.



Scheme 12 Use of IPr–copper complexes in carbonylative transformations.

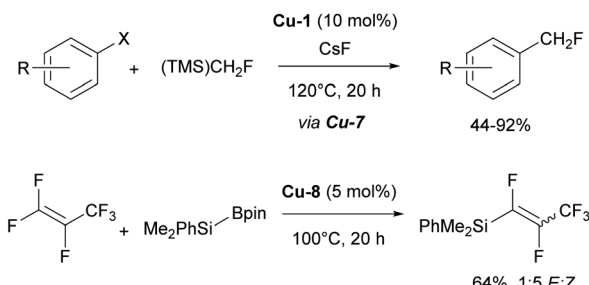
arylboronic ester nucleophiles and works efficiently with both primary and secondary alkyl iodide electrophiles (Scheme 12).<sup>88</sup> Another important contribution utilizing this chemistry was devoted to carbonylative silylation of alkyl halides, providing access to valuable acylsilane synthons.<sup>89</sup>

In 2015, Miura and Hirano reported a ligand-controlled regiodivergent Cu-catalyzed aminoboration of unactivated terminal alkenes. Interestingly, while using  $[\text{Cu}(\text{Xantphos})\text{Cl}]$ , boration occurs at the terminal position, however, the use of  $[\text{Cu}(\text{IPr})\text{Br}]$  provides access to borated product at internal positions with very good regioselectivity (Scheme 13a).<sup>90</sup> This methodology was later extended to include regiodivergent arylboration of the dienes using Cu/Pd catalytic system, where  $[\text{Cu}(\text{IPr})\text{Cl}]$  played a key role (Scheme 13b).<sup>91</sup>



Scheme 13 Examples of use of IPr–Cu complexes in borylation chemistry.





Scheme 14 The use of **IPr**-Cu complexes in fluorination and defluorination chemistry.

The Procter group reported on the borylative cross-coupling of allenes and imines using the  $[\text{Cu}(\text{IPr})\text{Cl}]/\text{KO}^{\prime}\text{Bu}$  catalytic system.<sup>92</sup> In this case, boration occurred selectively at the internal position of the allene, yielding branched  $\alpha,\beta$ -substituted- $\gamma$ -boryl homoallylic amines (Scheme 13c). This approach was further applied to the synthesis of quaternary  $\alpha$ -amino esters (Scheme 13d).<sup>93</sup>

In addition, it is important to highlight that the **IPr** ligand allowed for the isolation and characterization of the first copper difluoromethyl complex **Cu-7** (Fig. 4).<sup>94</sup> This important intermediate had never been isolated previously, despite copper-based catalytic systems being among the oldest and most widely used for the introduction of the  $\text{CHF}_2$  group. Following stoichiometric experiments, a catalytic version of this transformation was developed using  $[\text{Cu}(\text{IPr})\text{Cl}]$  as pre-catalyst and  $(\text{TMS})\text{CHF}_2$  as the difluoromethyl source (Scheme 14).<sup>94</sup>

Another noteworthy contribution in fluorine chemistry, featuring the **IPr**-Cu complex **Cu-8** (Fig. 4), is the defluorosilylation of fluoroalkene feedstocks providing access to fluorinated silanes.<sup>95</sup>

In closing this section, the synthesis of copper carbene–metal–amido (CMA) complexes, such as **Cu-9** (Fig. 4), which feature carbazole as an ancillary ligand is also worth mentioning. These complexes exhibited promising dual-emission properties and ultralong room-temperature phosphorescence (RTP), which hold great potential for the development of advanced RTP materials.<sup>96</sup>

### Gold catalysis and **IPr**

The report describing the synthesis and characterization of the first **IPr** gold complex dates to 2005.<sup>97</sup> The  $[\text{Au}(\text{IPr})\text{Cl}]$  complex **Au-1** (Fig. 5) was prepared by mixing free carbene with the

$[\text{Au}(\text{SMe}_2)\text{Cl}]$  precursor, in a simple ligand displacement reaction. These  $[\text{Au}(\text{NHC})\text{Cl}]$  complexes have quickly become widely used as pre-catalysts in gold-catalyzed transformations. Although much more cost-efficient and sustainable synthetic methods were developed to access NHC gold complexes,<sup>98</sup> this important report represents the onset of an avalanche of publications devoted to the use of these in various catalytic transformations. Notably, since the initial report, more than 800 publications have featured the **IPr**-gold core structure, establishing gold organometallic chemistry as a leading platform for the application of **IPr** as an ancillary ligand. While it is beyond the scope of this contribution to cover all these studies, we will focus on key milestones that have reinforced the central role of **IPr** in gold catalysis.

Upon gaining access to this new class of pre-catalysts, researchers naturally began exploring their potential in transformations previously mediated by phosphine–gold and NHC–copper complexes. In many instances, these investigations resulted in the development of milder reaction conditions, attributed to the unique steric and electronic properties of the NHC ligand, which enhance both the stability and reactivity of the active  $\text{LAu}^+$  species. Interestingly, the use of NHC–gold complexes has sometimes led to the discovery of entirely new catalytic reactions or significant alterations in reactivity compared to previously known systems. Notably, in most of these studies, **IPr**–gold complexes were the primary candidates tested and employed, underscoring the critical role of **IPr** in advancing gold-catalyzed transformations.

One particularly interesting example of a new catalytic reaction developed using gold NHC complexes, rather than the more traditional copper NHC complexes, is related to carbene-transfer reactions. Nolan and co-workers demonstrated that  $[\text{Au}(\text{IPr})\text{Cl}]$  not only catalyzed the expected cyclopropanation of olefins but also facilitated the formal insertion of carbenes into N–H and O–H bonds. Remarkably, the gold catalyst enabled unprecedented carbene insertion into the aromatic C–H bonds of styrene, benzene and toluene (Scheme 15a).<sup>99,100</sup> Among the many studies highlighting the enhanced reactivity of NHC–gold complexes, several early seminal reports stand out. Widenhoefer and co-workers reported that using  $[\text{Au}(\text{IPr})\text{Cl}]$  for the intramolecular hydroamination of *N*-alkenylacetamides allowed the reaction to proceed at lower temperatures than those required with phosphine-based analogues (Scheme 15b).<sup>101</sup> Similarly, the Toste group observed higher catalytic activity with **IPr**–gold complexes in the oxidative rearrangement of enynes compared to  $\text{PPh}_3$ -ligated gold complex (Scheme 15c).<sup>102</sup>

The Zhang group utilized  $[\text{Au}(\text{IPr})\text{NTf}_2]$  complex **Au-2** (Fig. 5) in the generation of  $\alpha$ -oxo gold carbenoids and their insertion into R–CO bonds (Scheme 15d).<sup>103</sup> Again, while an **IPr** complex facilitated this transformation, the related  $\text{PPh}_3$  analogue failed to do so.

In 2006 the Nolan group reported the isolation of well-defined cationic gold complex **Au-3** (Fig. 5), allowed to perform catalysis without activating  $\text{AgX}$  or  $\text{NaBAr}_4$  salts (Scheme 16).<sup>104</sup>

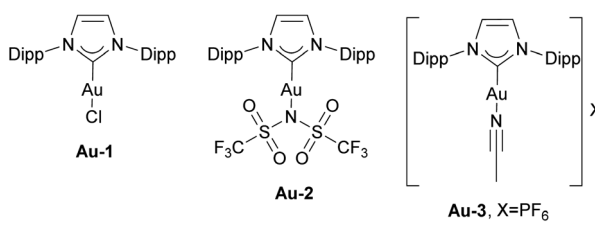
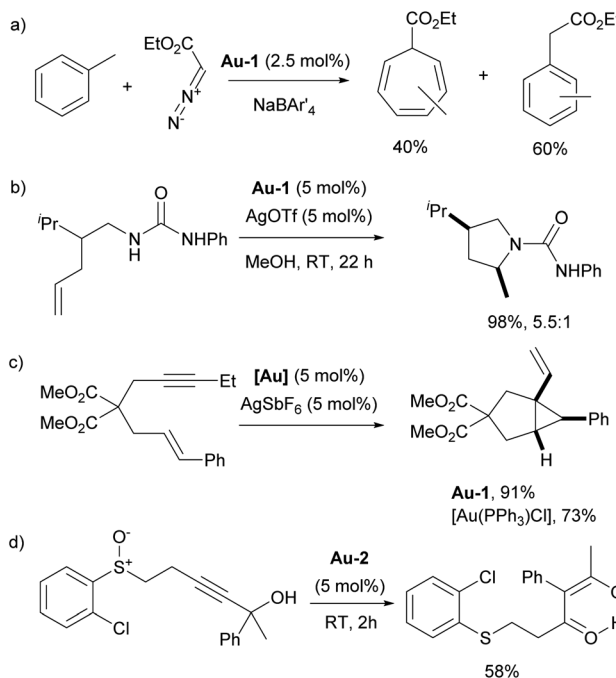
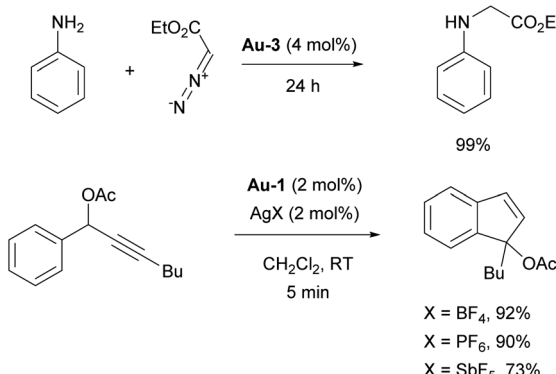


Fig. 5 Examples of the **IPr** gold complexes.



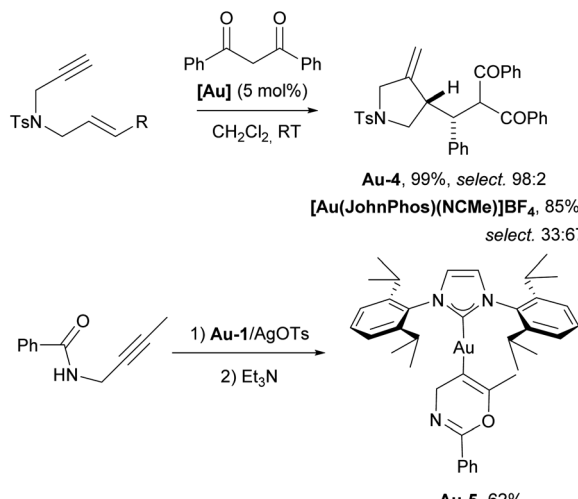


**Scheme 15** Early examples of the use of IPr–gold complexes exhibiting superior reactivity in comparison with phosphine–gold analogues.



**Scheme 16** The use of Au-3 in carbene insertion chemistry, and effect of counterion on hydroarylation.

The catalytic activity of **Au-3** (Fig. 5) was tested in carbene insertion of EDA and revealed the significant effect of the counterion on the reactivity. The same conclusion was drawn while using  $[\text{Au}(\text{IPr})\text{Cl}]/\text{AgX}$  catalytic system for novel tandem [3,3]-rearrangement-intramolecular hydroarylation to access indenes (Scheme 16; note that the SIMes-coordinated congener afforded a moderate yield, in contrast to **Au-1/AgX**).<sup>105</sup> The silver-free route, under **Au-6**/ $\text{HBF}_4 \cdot \text{Et}_2\text{O}$  (Scheme 18), supported by theoretical calculations is also efficient, where pre-catalyst activation is mediated by the  $\text{HBF}_4 \cdot \text{Et}_2\text{O}$  that acts as Brønsted acid.<sup>106</sup> In 2007, Ricard and Gagosz reported the synthesis of already mentioned IPr gold catalyst **Au-2** with weakly coordinating  $\text{NTf}_2$  moiety.<sup>107</sup> Although simultaneously reported by



**Scheme 17** The use of IPr–gold complex for intermolecular addition of carbon nucleophiles to 1,6-ene and isolation of the first gold–vinyl complex **Au-5**.

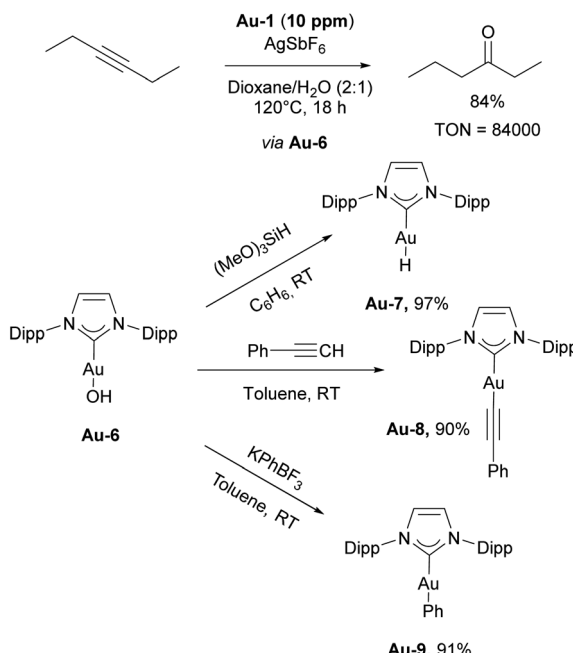
Zhang,<sup>103</sup> the synthesis and characterization of the complex was reported only in the former. These complexes demonstrated enhanced stability, particularly under ambient conditions, and proved highly active in a variety of gold-catalyzed transformations without the need of activating agent.<sup>107</sup> Based on these and related work, numerous reports dealing with the effect of the counterion in gold–NHC catalysis have appeared recently, revealing new aspects of the mechanisms of these transformations. Most of these reports once again utilized IPr–gold complexes as the “gold standard” for this chemistry.<sup>108–110</sup>

The remarkable ability of gold to activate  $\pi$ -bonds has long been recognized as one of its most distinctive features, accounting for the predominant focus on  $\pi$ -bond activation in gold-catalyzed reactions as seen above. Another important contribution in this area is the work of Echavarren in comprehensive studies of the gold-catalyzed intermolecular addition of carbon nucleophiles to 1,5- and 1,6-enynes.<sup>111</sup> From this report, it became clear that the reaction pathway could be directed by the auxiliary ligand, leading either to cyclopropane or carbene-site selectivity. The presence of NHC ligands, such as IPr, leads to carbene-site selectivity in most cases (Scheme 17).

The Hashmi group successfully isolated the first vinylgold complex **Au-5** (Scheme 17) using *N*-propargylcarboxamides as substrates and IPr as an auxiliary ligand on gold. This achievement provided direct evidence for the existence of these species in gold-catalyzed reactions with alkynes, which had been proposed as key intermediates but had never been isolated prior to this work.<sup>112</sup> Here again we have an example of the use of IPr to isolate reactive species.

The Nolan group reported on the use of  $[\text{Au}(\text{IPr})\text{Cl}]/\text{AgSbF}_6$  catalytic system for both formation of conjugated enols and enals, and acid-free alkyne hydration at ppm level catalyst loadings (Scheme 18, top).<sup>113</sup> In both cases, the presence of  $\text{H}_2\text{O}$  in the reaction mixture proved to be an important factor, allowing catalytic reaction to occur. Based on experimental and computational data, the reaction was hypothesized to proceed

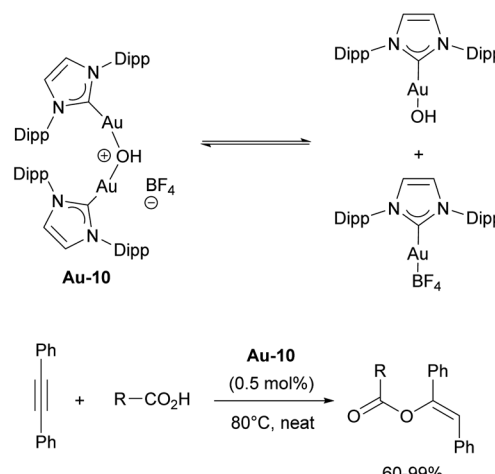




Scheme 18 Gold-catalyzed hydration of alkynes and reactivity of Au-5 hydroxide.

through the intermediate formation of  $[\text{Au}(\text{IPr})\text{OH}]$  species. Soon afterwards, complex **Au-6** was isolated using a simple procedure of mixing  $[\text{Au}(\text{IPr})\text{Cl}]$  with a hydroxide source. The obtained complex was found to be air- and moisture-stable, although highly basic and under the right conditions, very reactive.<sup>114</sup> The reactivity of this “golden synthon” was illustrated by reactions with various acids and compounds containing acidic C–H and O–H bonds, performed in air and at ambient temperature. Among several products accessible using this synthon, the gold hydride  $[\text{Au}(\text{IPr})(\text{H})]$  **Au-7**, gold aryl and alkynyl complexes **Au-8** and **Au-9** (Scheme 18) could be easily accessed. Furthermore, this development allowed for the use of gold hydroxide as a precatalyst for various transformations, using a Brønsted acid as activator to generate the  $\text{LAu}^+$  active species.<sup>115</sup> These silver-free protocols are of significant importance, as silver was found to not just act as an innocent activator but an actor for several transformations.<sup>116</sup> One of the most significant uses of the gold hydroxide is in the carboxylation of C–H bonds directly with  $\text{CO}_2$ .<sup>117</sup>

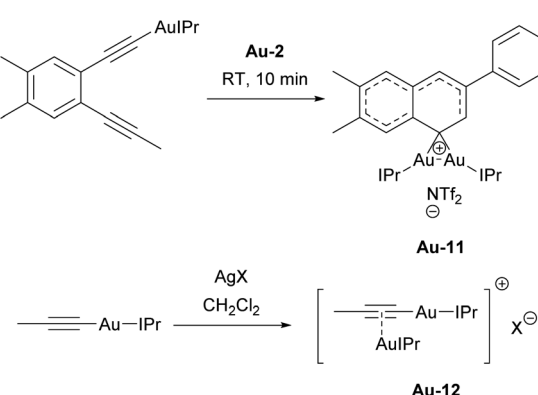
In the report describing silver-free protocols, the authors noted the formation of unreported species in the reaction mixture, which upon further investigation turned out to be a dinuclear species,  $[\{\text{Au}(\text{IPr})\}_2(\mu\text{-OH})]^+$ .<sup>115</sup> The isolated complex  $[\{\text{Au}(\text{IPr})\}_2(\mu\text{-OH})][\text{BF}_4^-]$  **Au-10** (Scheme 19) demonstrated excellent catalytic performance in the hydration of nitriles<sup>118</sup> and hydrophenylation of alkynes,<sup>119,120</sup> attributed to a “dual activation”<sup>121</sup> mechanism. This dual activation arises from the equilibrium between dinuclear complex and  $[\text{Au}(\text{IPr})\text{OH}]/[\text{Au}(\text{IPr})(\text{BF}_4^-)]$  pair, where the former functions as a Brønsted base and the latter operates as a Lewis acid (Scheme 19). This catalyst was later successfully employed in the hydroalkoxylation and hydrocarboxylation of alkynes.<sup>122,123</sup>



Scheme 19 Equilibrium of **Au-10** complex and its use in carboxylation of alkynes.

Just prior to reports on dinuclear gold catalysts, the Hashmi group explored various gold-catalyzed arylative cyclizations of 1,  $\alpha$ -dienes. This series of reports was of major importance in gold catalysis, as it shed light on and provided evidence for various important intermediates in gold-catalyzed reactions involving activation of  $\pi$ -bonds, confirming the dual catalytic role of gold.

In most cases, the **IPr** ligand was used as ancillary ligand, allowing for the detection or/and isolation of important intermediates. In 2012, Hashmi showed that formation of Au–C  $\sigma$ -bond plays an important role in the activation of triple bonds involving further  $\pi$ -binding of the second bond atom.<sup>124</sup> In the same report, the authors managed to isolate the first NHC-containing *gem*-diaurated aryl species **Au-11** and provided the rationale for its role in the catalytic cycle (Scheme 20). The follow-up report provided further compelling evidence for the dual activation role of gold and the involvement of gold vinylidene intermediates in the formation of dibenzopentalenes from arene-1,2-diene.<sup>125</sup> Finally, those  $\sigma, \pi$ -alkyne gold acetylides complexes were isolated and fully characterized, including X-ray diffraction on single crystals, which provided insights in their structure (Scheme 20). Those complexes were probed as on-



Scheme 20 Isolation of important intermediates **Au-11** and **Au-12**.



cycle catalysts for hydroarylating aromatization and proved efficient without additives.<sup>126</sup> In contrast to these findings, the Echavarren group successfully isolated several  $\sigma,\pi$ -digold alkyne complexes bearing the **IPr** ligand. Following mechanistic investigations, including both experimental and theoretical studies, they concluded that these complexes represent “dead ends” in gold catalysis involving enynes.<sup>127</sup>

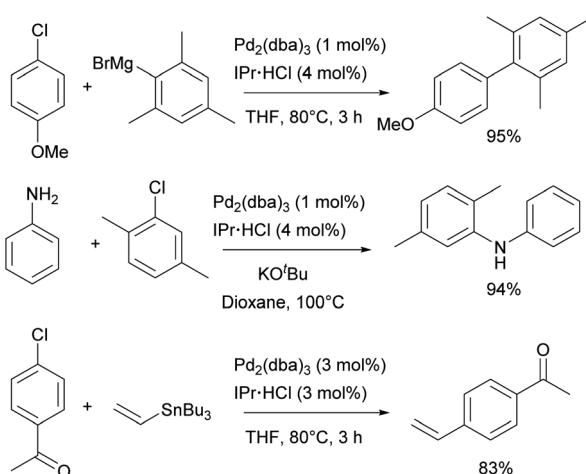
With ongoing advances in gold catalysis, **IPr** has emerged as the preferred ligand for NHC–gold catalytic systems, reinforcing its position as one of the most widely employed ligands in this field. Recent applications of **IPr** include a variety of transformations including the domino<sup>128</sup> and cascade cyclization,<sup>129</sup> cycloaddition,<sup>130</sup> and annulation<sup>131</sup> reactions, as well as for hydrofluorination<sup>132</sup> and hydration<sup>133</sup> of triple bonds. The versatility displayed by **IPr** extends even to more unconventional areas of gold chemistry, including the encapsulation<sup>134</sup> of gold complexes and their use in energy transfer photocatalysis.<sup>135,136</sup>

### Palladium catalysis and **IPr**

Catalytic studies involving **IPr** in palladium catalysis began shortly after the discovery of the ligand itself, in 1999. The initial reports focused on the amination of aryl halides<sup>13</sup> and the Kumada–Tamao–Corriu coupling,<sup>14</sup> both utilizing *in situ* generated catalysts from  $\text{Pd}_2(\text{dba})_3$  and imidazolium salts as precursors. This approach was later extended to Hiyama and Stille couplings, using  $\text{Pd}(\text{OAc})_2$  as the palladium source (Scheme 21).<sup>137,138</sup> After the development of such efficient protocols for those transformations, the next significant development was the design of  $\text{Pd}/\text{NHC}$  well-defined complexes.

In 2002, the Nolan group introduced two families of the well-defined  $\text{Pd}/\text{NHC}$  precatalysts – NHC palladium  $\mu$ -chlorobridged dimers  $[\text{Pd}(\text{NHC})\text{Cl}_2]_2$ <sup>139</sup> and NHC palladium allyl complexes  $[\text{Pd}(\text{NHC})(\text{allyl})\text{Cl}]$ .<sup>140</sup> Subsequently, both of these families played a substantial role in further advancing the area of NHC–palladium catalysis.

In particular,  $[\text{Pd}(\text{IPr})\text{Cl}_2]_2$  (**Pd-1**, Fig. 6) showed remarkable catalytic activity in various aryl halide aminations, including



Scheme 21 Some early examples of **IPr** ligand use in palladium chemistry.

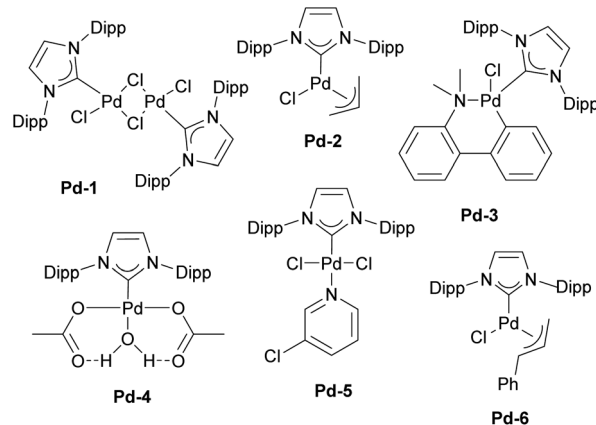


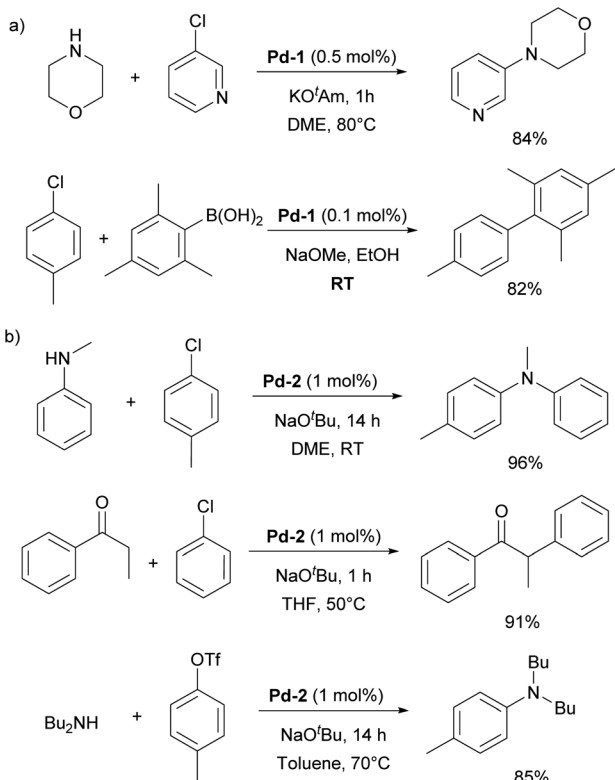
Fig. 6 Selected examples of **IPr**–palladium complexes used in catalysis.

very challenging versions and operating under surprisingly mild reaction conditions, *i.e.* without the need for anhydrous and anaerobic conditions (Scheme 22a).<sup>139</sup> Subsequently, this catalyst was employed in room-temperature Suzuki–Miyaura couplings,<sup>141,142</sup> and a recent comprehensive study on its activation has been published.<sup>143</sup> This study included a direct comparison with various other precatalysts developed later and revealed that this previously “overlooked” family of pre-catalysts remains among the most active. Consequently, the authors suggested that these pre-catalysts should be considered as a preferred option in catalytic applications.

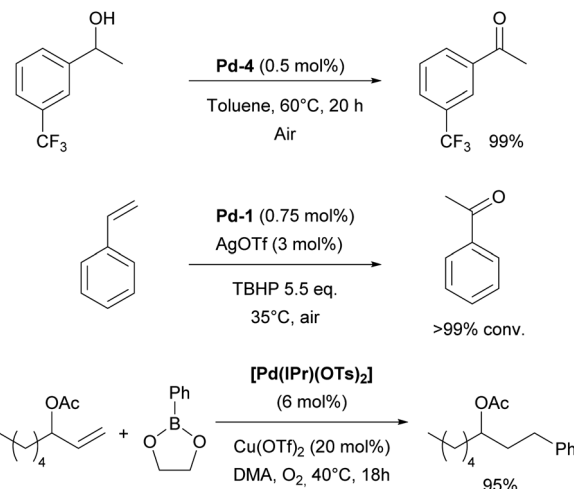
$[\text{Pd}(\text{NHC})(\text{allyl})\text{Cl}]$  complexes, being air- and moisture-stable compounds, were successfully tested in the arylation of ketones, Suzuki–Miyaura and Buchwald–Hartwig cross-coupling reactions.<sup>140,144,145</sup> Later on, a more detailed study on these reactions was reported revealing a very high efficiency of  $[\text{Pd}(\text{IPr})(\text{allyl})\text{Cl}]$  (**Pd-2**, Fig. 6) (Scheme 22b).<sup>146</sup>

Since then, considerable amount of research has focused on optimizing the structure of NHC–palladium precatalysts to develop more readily activated and efficient complexes. Numerous families of precatalysts have been synthesized and evaluated, with varying degrees of success in terms of catalytic efficiency. However, it is noteworthy that precatalysts containing **IPr** as an ancillary ligand are almost always among the first to be synthesized and tested, serving as a benchmark in comparative studies.

One of such families was NHC palladacycles, which combined the stability of the metallacycle scaffold with strong  $\sigma$ -donating properties of the NHC ligands. In a series of reports **IPr** congener **Pd-3** (Fig. 6) showed high catalytic activity in various room temperature cross-coupling reactions, including Suzuki–Miyaura coupling with hindered (di)ortho-substituted aryl chlorides (Scheme 23).<sup>147,148</sup> A more comprehensive study on Suzuki–Miyaura,  $\alpha$ -ketone arylation and dehalogenation reactions provided efficient protocols for the use of these precatalysts, with **IPr** complex **Pd-3** being the most efficient.<sup>149</sup> The Morandi group recently used the same precatalyst for C–S and C–P bonds metathesis by reversible arylation.<sup>150</sup>



Scheme 22 Utilization of Pd-1 and Pd-2 in cross-coupling reactions.

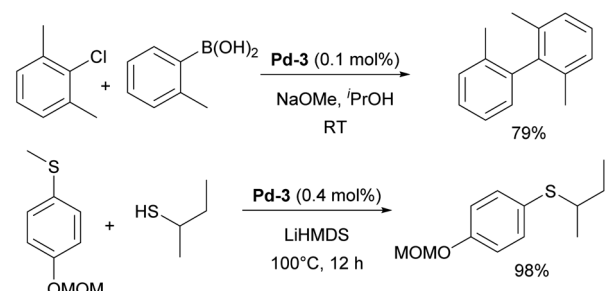


Scheme 24 Use of IPr acetato and tosylato palladium complexes in catalysis.

a substrate.<sup>155</sup> This precatalyst was also employed in the oxidative 1,1-diarylation of terminal olefins<sup>156</sup> and oxidative Heck coupling.<sup>157</sup>

In 2006, two of the most successful and widely utilized families of NHC-palladium precatalysts were introduced. In both cases, IPr-ligated precatalysts were synthesized and evaluated in a variety of reactions to demonstrate their robustness, versatility and efficiency. The Organ group pioneered the use of 3-chloropyridine as a “throw-away” ligand, resulting in the development of PEPPSI precatalysts, which stands for Pyridine-Enhanced Precatalyst Preparation, Stabilization, and Initiation.<sup>158</sup> These precatalysts can be produced on a large scale under ambient conditions and are highly bench-stable, allowing for long-term storage. Initially, these catalysts were prepared using a non-environmentally friendly procedure with 3-chloropyridine as the solvent. However, a more atom-economical and environmentally friendly method has recently been developed.<sup>159</sup> The well-defined IPr-Pd-PEPPSI complex **Pd-5** (Fig. 6) was first tested in Negishi reactions for C(sp<sup>3</sup>)-C(sp<sup>3</sup>) coupling, as well as in Suzuki-Miyaura couplings with boronic acids and trifluoroborates. Notably, the well-defined system exhibited a much faster initial reaction rate and significantly higher turnover numbers (TON) compared to *in situ* generated catalysts. This complex alone appears in more than 360 publications since its discovery, including reports featuring its implementation in Buchwald-Hartwig,<sup>160</sup> Negishi<sup>161</sup> and Kumada-Tamao-Corriu<sup>162</sup> cross-couplings (Scheme 25). The non-chlorinated version of **Pd-5** has recently been used in a mechanistic study devoted to R-NHC coupling under catalytic conditions,<sup>163</sup> which was shown to dictate whether the so-called NHC-connected or disconnected mode of catalysis is at play in particular transformations.<sup>164</sup>

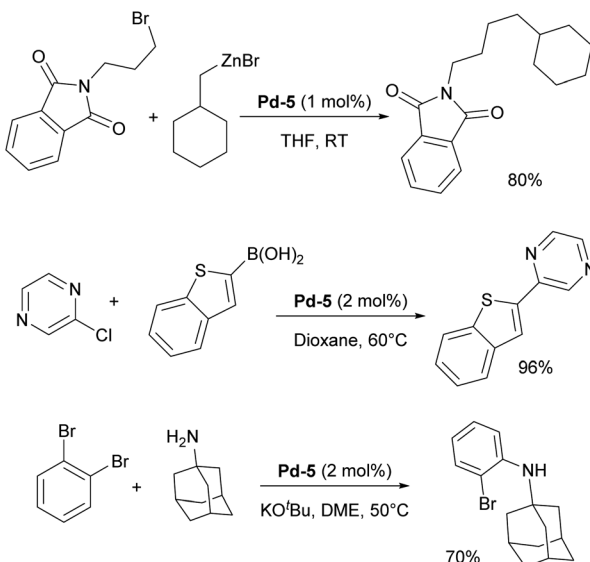
The Nolan group developed a modified version of [Pd(NHC)(allyl)Cl] complexes (let us call these, the second generation Pd-allyl family) by altering the substituents on the allyl moiety.<sup>165</sup> It was found that the incorporation of a phenyl group at the terminal position of the allyl ligand facilitated



Scheme 23 The use of Pd-3 pre-catalyst in catalysis.

During the same period, the Sigman group worked on the palladium-catalyzed aerobic oxidation of alcohols. After successfully using the aforementioned [Pd(IPr)Cl<sub>2</sub>]<sub>2</sub> dimer (**Pd-1**) for oxidative kinetic resolution of secondary alcohols<sup>151</sup> and based on mechanistic insights, they introduced IPr-palladium-acetato complex (**Pd-4**, Fig. 6) for aerobic oxidation of alcohols (Scheme 24).<sup>152</sup> The acetate ligand plays a key role in facilitating intramolecular deprotonation, which enhances catalytic efficiency. Further in-depth mechanistic investigations and screenings<sup>153</sup> led to significant advances in this field.<sup>154</sup> The introduction of the tosylate congener [Pd(IPr)(OTs)<sub>2</sub>] obtained *in situ* from **Pd-1** and AgOTf, permitted the use of *tert*-butyl hydroperoxide (TBHP) as the oxidant instead of copper additives in the Wacker oxidation of styrenes, leading to high conversion rates and selectivity for acetophenone as



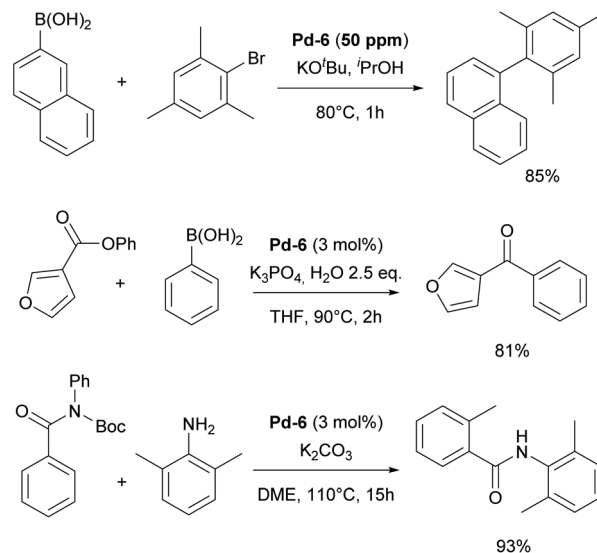


**Scheme 25** Representative examples of the **IPr**–Pd–PEPPSI complex (**Pd-5**) employed in diverse cross-coupling reactions.

faster activation of the precatalysts, leading to enhanced catalytic activity across a broad range of transformations. Note that this lesson learned in Pd–NHC catalyst development has been adapted to Pd–Buchwald phosphine by Colacot and co-workers at Johnson Matthey.<sup>166</sup>

The resulting NHC Pd–cinnamyl (and crotyl and prenyl) complexes, particularly  $[\text{Pd}(\text{IPr})(\text{cinnamyl})\text{Cl}]$  (**Pd-6**, Fig. 6), exhibited exceptional efficiency, enabling Suzuki–Miyaura couplings with challenging substrates at very low catalyst loadings and at room temperature. In some cases, reactions were successfully conducted with as little as 50 ppm of catalyst, achieving 93% yield within 3 hours, demonstrating the remarkable efficiency of the developed catalytic system (Scheme 26). The **Pd-6** catalyst demonstrated exceptional reactivity in Suzuki–Miyaura couplings with non-traditional electrophiles, including aryl esters and amides, as reported by the Szostak group.<sup>167,168</sup> In both instances, the developed protocol enabled the efficient synthesis of diaryl ketones with a broad substrate scope and high yields, utilizing a commercially available palladium precatalyst. Studying the effect of the substitution on the backbone of the N-heterocyclic ring of **Pd-6** in the Suzuki–Miyaura coupling experimentally and through DFT calculations provided crucial insights into the activation pathway of precatalysts and reactivity of complexes.<sup>169</sup> Additionally, this catalyst was employed in the first general method for the transamidation of secondary carboxamides, significantly expanding the scope of amide N–C bond cross-coupling reactions.<sup>170,171</sup> In this arena, it should be clearly stated that Pd–phosphine complexes have been found lacking in terms of catalytic effectiveness and that Pd–NHC systems rule the day in this area.

The pursuit of more efficient, robust, universal, and sustainable NHC–palladium precatalysts remains an ongoing area of research, leading to the development and evaluation of



**Scheme 26** Representative examples of the **IPr**–palladium cinnamyl complex (**Pd-6**) employed in various cross-coupling reactions.

numerous new pre-catalysts, such as the  $[\text{Pd}(\text{NHC})(\text{acac})\text{Cl}]$ <sup>172</sup> and  $[\text{Pd}(\text{NHC})(\text{n}^3\text{-1}^4\text{Bu-indenyl})\text{Cl}]$  systems.<sup>173</sup> Notably, the **IPr** ligand continues to serve as a benchmark for comparison within these novel structures, underscoring its pivotal role in NHC palladium catalysis. However, following the success of highly efficient NHC–Pd–cinnamyl and NHC–Pd–PEPPSI pre-catalysts, researchers have increasingly focused on modifying the NHC ligand itself to further enhance catalytic efficiency and selectivity, especially for more challenging substrates. This shift has led to the development of various NHC ligands inspired by **IPr**, which will be discussed in the following section, providing insights into the design, evolution, and applications of these new NHC ligands in catalysis.

### The far-reaching influence of the **IPr** structure

As could be seen from the previous sections, the role of **IPr** as an indispensable ligand in the vast array of NHCs is evident. The use of the ligand consistently enhances stability, catalytic activity, and selectivity in various catalytic processes featuring a variety of transition metals, making it a privileged construct in the design of efficient catalytic systems. The versatility of **IPr** in facilitating a wide range of transformations, from cross-couplings to hydroaminations and metathesis, underscores its adaptability to different metals and reaction conditions. As we look to the impact (past and future) of **IPr** on NHC ligand design, the following section will offer an overview of the evolution of **IPr**-inspired ligands, discussing the emerging modifications that aim to move the boundaries of catalytic performance forward and meet the demands for increasingly efficient and sustainable transformations.<sup>174</sup>

Over the course of the previous two decades, substantial efforts have been made by several research groups to exploit the unique properties that are inherent to the **IPr** architecture, to design and synthesize new families of NHC ligands, with the



goal of exploring their potential in catalysis. The closest analogue to **IPr** is its saturated counterpart, (1,3-bis(2,6-diisopropylphenyl))imidazolidin-2-ylidene (**SIPr**). Arduengo reported the synthesis of the free **SIPr** in the same year as when **IPr** ligand was introduced,<sup>175</sup> so it cannot be said that the development of **SIPr** was directly inspired by **IPr**. However, the **IPr**-inspired modifications, we feel, has led to the design of four major NHC architectures: **IPr\*** (1,3-bis[2,6-bis(diphenylmethyl)-4-methylphenyl] imidazole-2-ylidene, **IPr\*\*** (1,3-bis(2,6-di(*p*-*tert*butylphenyl)methyl-4-methylphenyl)imidazole-2-ylidene, **IPr#** (1,3-bis(2,4,6-tribenzhydrylphenyl)-1*H*-imidazole-2-ylidene), and all members of the **ITent** (Tent = tentacular) family (Fig. 7).

In the following section, we will highlight selected examples of applications of these **IPr**-inspired NHCs in catalysis. The **IPr** and **SIPr**, being structurally similar, have often been examined side-by-side in many of the aforementioned-reactions. In most cases, **IPr** demonstrated somewhat better catalytic activity, stability, and/or selectivity. However, there are several notable instances where **SIPr** outperformed its counterpart. Saturated NHCs occupy a unique position among ligands in ruthenium metathesis, as even slight variations in the electronic and steric properties of NHC ligands can significantly impact reactivity.<sup>28</sup> Shortly after the development of **SIPr**, it was shown that complexes containing **SIPr** exhibited substantially higher catalytic activity, with 6- and 20-fold increases in TON and TOF, respectively, for the metathesis of 1-octene, compared to the (*S*) **IMes** catalyst, which was the standard at the time (Scheme 27).<sup>176</sup> Similarly, **SIPr**-based complexes have been found to be highly active in acyclic diene metathesis polymerization (ADMET).<sup>177</sup> In palladium chemistry, **SIPr**-ligated

complex **Pd-7** allowed *N*-arylation with aryl chlorides at room temperature in minutes.<sup>178</sup> **[Au(SIPr)F]** complex was used to detect and isolate  $\beta$ -(fluorovinyl)gold complexes for the first time, showing the reversible nature of their formation (Scheme 27). This observation resulted in the first gold-catalyzed hydrofluorination of alkynes under mild conditions.<sup>179</sup> Interestingly, **SIPr** was also a ligand of choice in one of the widely known studies by the Fokin group, where the mechanism of copper-catalyzed azide–alkyne cycloaddition (CuAAC) was explored and the ligand used to stabilize dinuclear copper intermediates.<sup>180</sup>

One of the most influential classes of NHCs inspired by the **IPr** scaffold is the **ITent** (tentacular NHCs) family, which includes **IPent** (1,3-bis(2,6-di(3-pentyl)phenyl)imidazole-2-ylidene), **IHept** (1,3-bis(2,6-di(4-heptyl)phenyl)imidazole-2-ylidene), and **INon** (1,3-bis(2,6-di(5-nonyl)phenyl)imidazole-2-ylidene). Although **IPent** was first described by the Organ group,<sup>181</sup> its synthesis was not reported in the literature until the Nolan group disclosed its detailed synthetic protocol.<sup>182</sup> The **IPent** PEPPSI complex **Pd-8** demonstrated exceptional activity in Suzuki–Miyaura cross-coupling reactions, particularly in the synthesis of challenging *ortho*-substituted biaryls, catalytically outperforming its **IPr** counterpart (Scheme 28).<sup>181</sup> Additionally, the **IPent** cinnamyl complex **Pd-9** was also found to be highly active for the same transformation, while the **IHept** congener **Pd-10** exhibited the highest reactivity in Buchwald–Hartwig amination (Scheme 28).<sup>182</sup> However, in both case studies, the increased steric bulk of **INon** did not result in higher catalytic activity, offering valuable insights into the limitations of the “bulky yet flexible” concept in NHC design.

Subsequently, the Organ group discovered that introducing halide atoms on the backbone (C4 and C5 positions) of the NHC

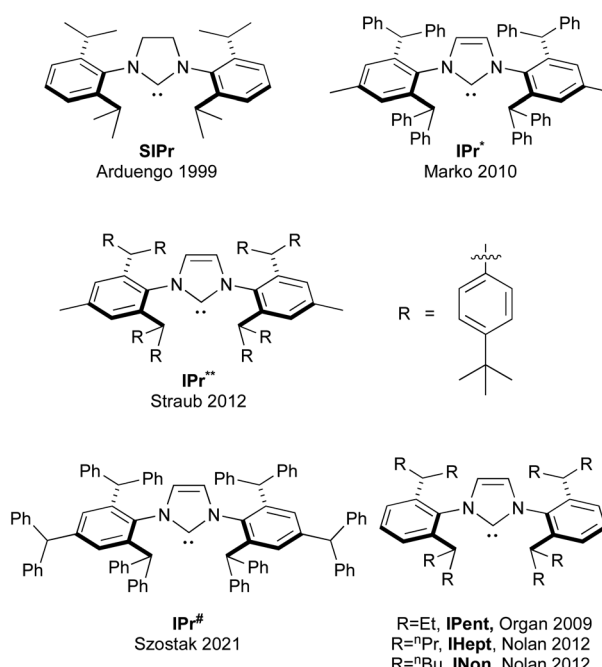
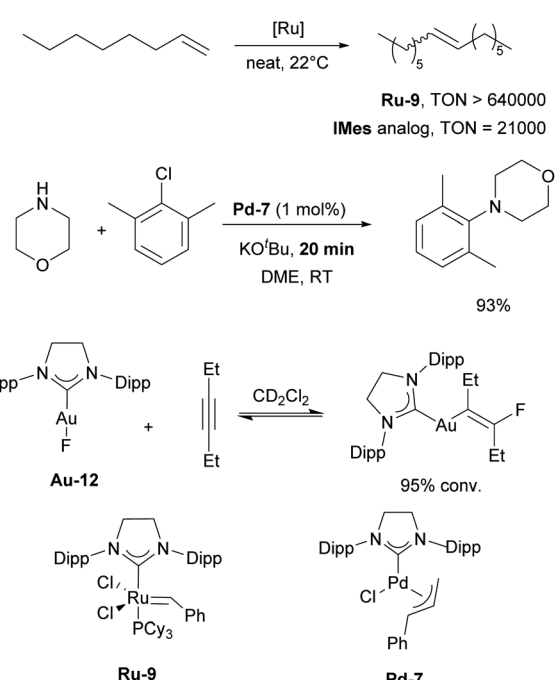
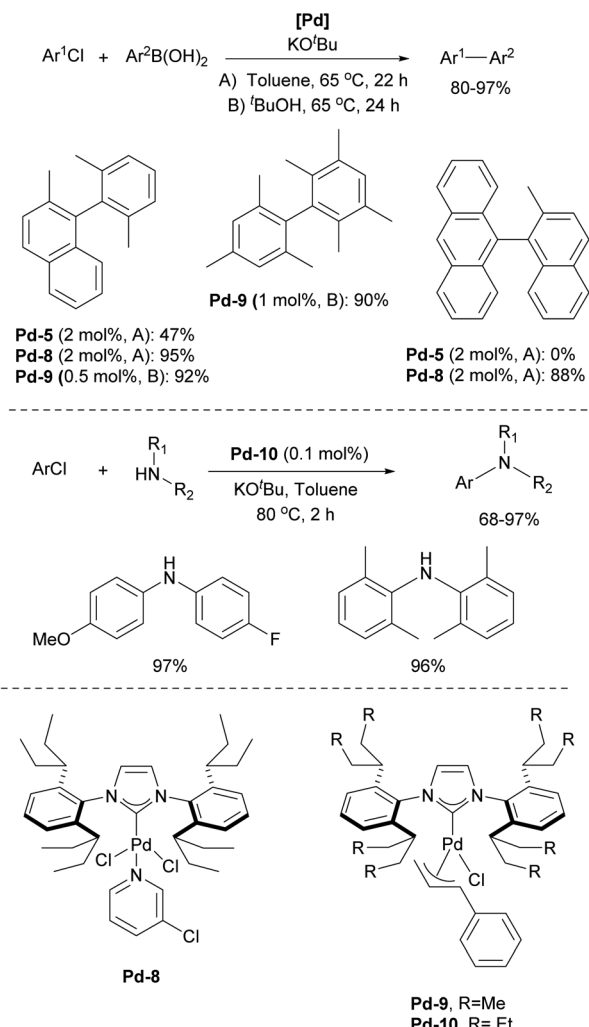


Fig. 7 **SIPr** and other NHC ligands inspired and developed based on the **IPr** structure.



Scheme 27 Examples of the use of **SIPr** in catalysis.

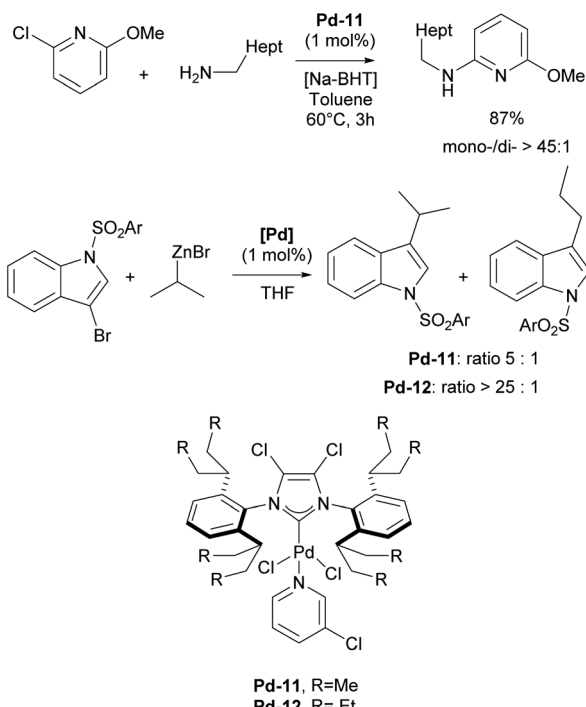


Scheme 28 Use of ITent family ligands in palladium chemistry.

ligands in the **ITent** family, could enhance catalytic activity. In particular, Pd-PEPPSI-IPent<sup>Cl</sup> **Pd-11** was found to be an excellent precatalyst for selective monoarylation of primary amines with aryl halides, affording monoarylation products in 49–99% yields (Scheme 29).<sup>183</sup> The IHept<sup>Cl</sup> analog of **Pd-12** was also utilized in the selective coupling of secondary alkyl zinc reagents and heteroaryl bromides, accelerating the reductive elimination, which leads to minimal amount of rearranged products caused by migratory insertion.<sup>184</sup>

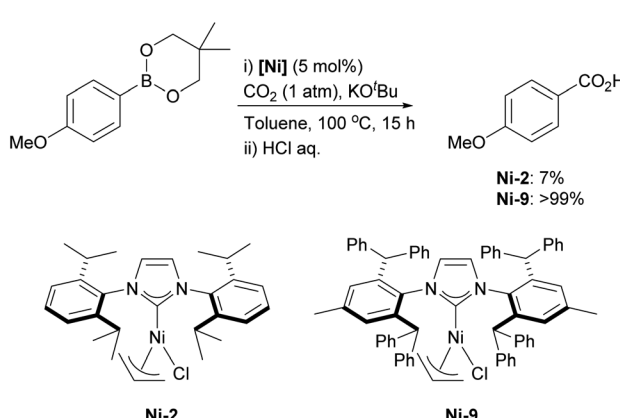
The higher reactivity of the Pd-PEPPSI-IHept<sup>Cl</sup> precatalyst, in contrast to Pd-PEPPSI-IPent<sup>Cl</sup>, was attributed to the increased bulkiness of IHept<sup>Cl</sup>, which substantially affects the competitive  $\beta$ -hydride elimination when secondary alkyl zinc reagents are employed (Scheme 29).

The synthesis of the **IPr\*** imidazolium salt was first reported by Markó and coworkers, following a modified route akin to that of the **IPr** imidazolium salt.<sup>185</sup> The process involves dialkylation of *p*-toluidine with benzhydrol in the presence of concentrated HCl and ZnCl<sub>2</sub> to afford the corresponding aniline, which, after treatment with glyoxal, yields the diimine intermediate. Finally, the **IPr\***-HCl salt is obtained by refluxing the diimine and



Scheme 29 Use of backbone-chlorinated IPent and IHept ligands in catalysis.

paraformaldehyde in chloroform in the presence of ZnCl<sub>2</sub>. **IPr\*** is significantly more sterically bulky than **IPr**, which leads to notable differences in its structural and catalytic properties. A representative example is the carboxylation of organoboronates, catalyzed by the  $[\text{Ni}(\text{IPr}^*)(\eta^3\text{-allyl})\text{Cl}]$  complex.<sup>186</sup> Nolan and coworkers demonstrated that nickel precatalyst **Ni-9** affords the corresponding carboxylic acid in quantitative yield, whereas the  $[\text{Ni}(\text{IPr})(\eta^3\text{-allyl})\text{Cl}]$  complex (**Ni-2**) yielded only 7% of the product (Scheme 30). The superior performance of the bulkier **IPr\***-coordinated nickel complex **Ni-9**, compared to **Ni-2**, may be attributed to the stabilization of reactive intermediates or the acceleration of a key step (reductive elimination, most likely) along the reaction pathway. Although DFT studies provided

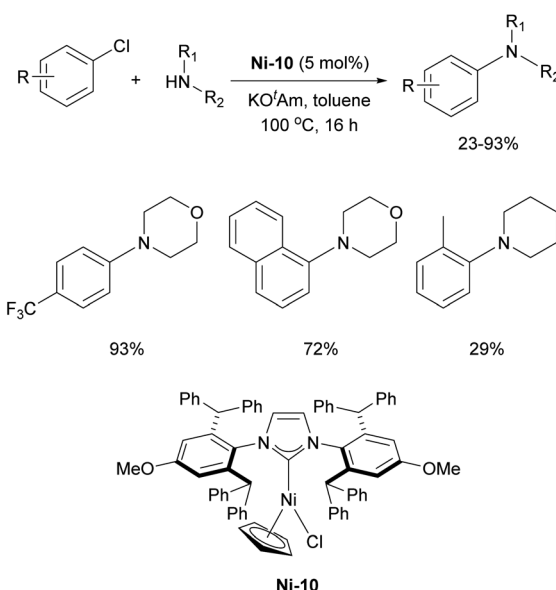
Scheme 30 Higher activity of **IPr\***-Ni precatalyst in comparison with **IPr**-Ni congener.

valuable mechanistic insights, they were insufficient to fully explain the necessity of the sterically bulky NHC for achieving high catalytic activity.<sup>187</sup>

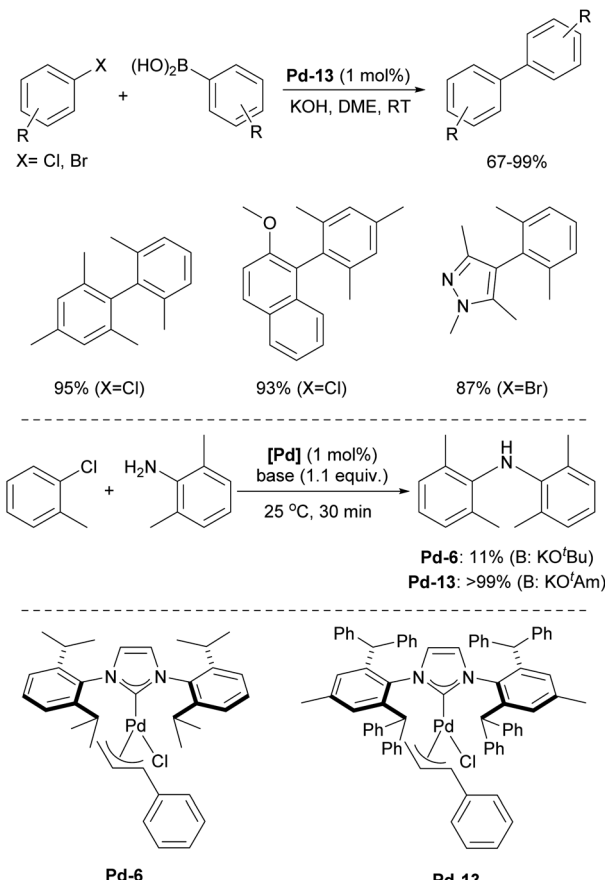
Further increasing the steric bulk of **IPr\*** by introducing an OMe group at the *para*-position was found to have a positive effect on Ni-catalyzed C–N coupling between morpholine and 1-chloro-4-methylbenzene.<sup>188</sup> It was postulated that the enhanced steric bulk of **IPr\*OMe** stabilized the  $[\text{Ni}^0(\text{NHC})]$  active species, preventing their rapid decomposition. However, this increased bulkiness compromised the ligand's flexibility, limiting the incorporation of sterically hindered aryl halides near the metal center, which consequently could not be efficiently converted into the corresponding products (Scheme 31).

One of the most notable examples of the use of the **IPr\*** architecture in catalysis is related to palladium chemistry. Shortly after the introduction of **IPr\***, the Nolan group synthesized the  $[\text{Pd}(\text{IPr}^*)(\text{cin})\text{Cl}]$  complex, analogous to the successful  $[\text{Pd}(\text{IPr})(\text{cin})\text{Cl}]$  and investigated its catalytic performance in Suzuki–Miyaura cross-coupling reactions, particularly with challenging tetra-*ortho*-substituted biaryls. Remarkably, this palladium precatalyst, featuring the sterically bulky yet flexible **IPr\*** ligand, performed efficiently with sterically hindered substrates, achieving 67–99% yields at room temperature.<sup>189</sup> Noteworthy examples include the reaction between mesityl chloride and 2,6-dimethylbenzene boronic acid, 1-chloro-2-methoxynaphthalene and mesityl boronic acid, as well as 4-bromo-1,3,5-trimethyl-1*H*-pyrazole and 2,6-dimethylbenzene boronic acid (Scheme 32).

Given the remarkable reactivity of **Pd-13** (Scheme 32) in Suzuki–Miyaura coupling, it was soon tested in Buchwald–Hartwig amination. Similarly, **Pd-13** demonstrated high catalytic activity, even at very low catalyst loadings (0.05 mol%), affording a broad scope of products.<sup>190</sup> Deactivated and heteroaryl chlorides were reactive under these conditions, and the typically challenging dibutylamine also underwent successful

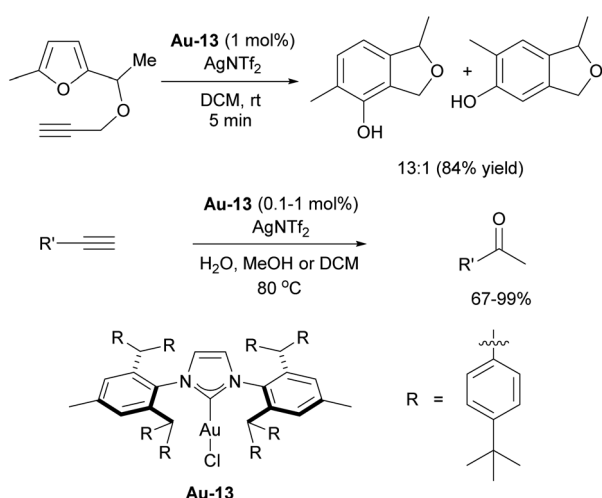


Scheme 31 **Ni-10** precatalyst in Buchwald–Hartwig amination.



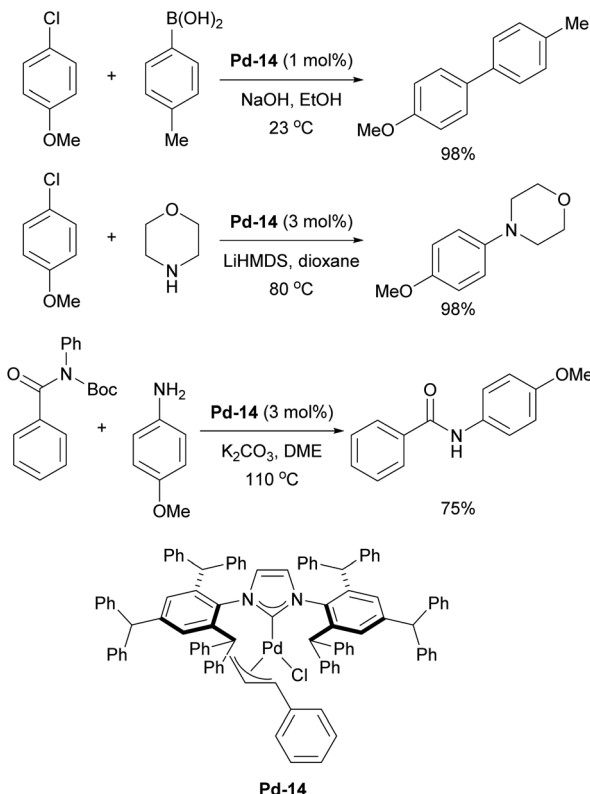
Scheme 32 Performance of **Pd-8** in Suzuki–Miyaura and Buchwald–Hartwig cross-coupling reactions.

coupling, although a slightly higher loading of **Pd-13** (0.1 mol%) was required to achieve a 58% yield. This is noteworthy compared to other studies that required higher catalyst loadings.<sup>191</sup> **Pd-13** was also evaluated in solvent-free Buchwald–Hartwig cross-coupling reactions of unactivated aryl chlorides



Scheme 33 Catalytic activity of **Au-13** in phenol synthesis.





**Scheme 34** Examples of use of **IPr#** in palladium-catalyzed cross-coupling reactions.

with secondary and tertiary amines, yielding the corresponding products in up to >99%.<sup>192</sup> When comparing the reactivity of precatalysts **Pd-13** and its **IPr** analogue, **Pd-6**, the former achieved >99% conversion to the coupling product, while **Pd-6** provided only 11% conversion (Scheme 32).

Once again, it is evident that the increased steric bulkiness of **IPr\*** could permit to overcome some of the catalytic limitations of the **IPr** ligand. Subsequently, **Pd-13** was also employed in the *S*-arylation of unactivated arylsulfoxides, where it again outperformed **Pd-6**. In the reaction between methylphenylsulfoxide and *p*-bromotoluene, **Pd-13** afforded 85% conversion, compared to just 9% with **Pd-6** as the precatalyst.<sup>193</sup>

Straub and coworkers reported an even bulkier version of **IPr\***, namely, **IPr\*\***, which is decorated by eight *tert*-butyl groups at *para*-positions of phenyl substituents on the wingtips (Fig. 7). Despite a substantial effort needed to synthesize this ligand and its relatively poor catalytic activity in palladium catalysis, **IPr\*\*** is uniquely useful catalyst due to its increased bulkiness.<sup>194</sup> It provides excellent stabilization to the metal center, which was confirmed by stabilizing a gold–arene complex, originating from the C–B cleavage of one of the aryl groups of  $\text{BArF}_{24}$  and gold–silver intermediate allegedly formed during activation of gold complexes with silver salts.<sup>195,196</sup>

Additionally, **IPr\*\*** gold complexes have shown promising catalytic activity in several gold-catalyzed transformations including phenol synthesis and hydration of alkynes (Scheme 33).<sup>197</sup> The benefits of further extending the steric properties along this direction appeared to have reached its optimum

peak, until recent reports inspired by the invaluable applications of **IPr** and **IPr\*** in catalysis, where Szostak and coworkers have developed a new ligand, **IPr#**, which was synthesized using a procedure similar to that of **IPr\***.<sup>198,199</sup> Structural analysis of  $[\text{Au}(\text{NHC})\text{Cl}]$  complexes demonstrated that **IPr#** is bulkier than **IPr\***, but slightly less sterically hindered than **IPr\*\***. This ligand has been successfully applied in various palladium-catalyzed cross-coupling reactions, using the cinnamyl precatalyst **Pd-14** (Scheme 34). It proved efficient in Suzuki–Miyaura, Buchwald–Hartwig, and transamidation reactions (Scheme 34).<sup>198</sup> Additionally, the Ghosh group utilized **IPr#** to synthesize silver and copper chloride and bromide complexes, which were successfully employed in  $\text{A}^3$  (amine–aldehyde–alkyne) coupling reactions.<sup>200</sup> The chase here continues and the original design of the **IPr** appears to still hold promise for further improvements in catalytic performances.

## Conclusions

The **IPr** ligand has been shown as a transformative element in the field of N-heterocyclic carbene (NHC) chemistry, profoundly influencing the development of organometallic catalysis across a wide range of metals and reactions. Its unique combination of steric bulk and electronic properties has not only led to enhanced stability and reactivity of metal complexes but has also enabled catalytic transformations that were previously challenging or inaccessible. Over the past 25 years, **IPr** has been instrumental in advancing both the fundamental understanding of NHC ligands and their practical applications in catalysis, especially in the chemistry of transition metals.

Moreover, the versatility and robustness of **IPr** have inspired the development of new NHC ligands tailored to specific catalytic needs, broadening the scope of NHC-based chemistry. As research continues to evolve, the **IPr** framework remains a cornerstone in the design of next-generation catalysts, shaping future advances in catalysis and materials science. Its lasting impact on the field underscores its significance as a privileged/benchmark ligand, ensuring its continued relevance in modern chemistry and still holds surprises in the evolution and understanding of modern catalyst design.

## Data availability

No primary research results, software or code have been included and no new data were generated or analysed as part of this review.

## Author contributions

VAV, LPZ and SPN wrote the manuscript and have given approval to the final version.

## Conflicts of interest

There are no conflicts to declare.



## Acknowledgements

The FWO is gratefully acknowledged for support of this work as are collaborators who have greatly contributed to the development of the area and whose names can be found in the references.

## Notes and references

- D. M. Flanigan, F. Romanov-Michailidis, N. A. White and T. Rovis, *Chem. Rev.*, 2015, **115**, 9307–9387.
- N-Heterocyclic Carbenes in Organocatalysis*, ed. A. T. Biju, Wiley-VCH, Weinheim, 2019.
- P. L. Arnold and I. J. Casely, *Chem. Rev.*, 2009, **109**, 3599–3611.
- C. A. Smith, M. R. Narouz, P. A. Lummis, I. Singh, A. Nazemi, C.-H. Li and C. M. Crudden, *Chem. Rev.*, 2019, **119**, 4986–5056.
- M. Koy, P. Bellotti, M. Das and F. Glorius, *Nat. Catal.*, 2021, **4**, 352–363.
- I. Ott, in *Advances in Inorganic Chemistry*, ed. P. J. Sadler and R. van Eldik, Academic Press, 2020, vol. 75, pp. 121–148.
- A. Doddì, M. Peters and M. Tamm, *Chem. Rev.*, 2019, **119**, 6994–7112.
- A. Igau, H. Grutzmacher, A. Baceiredo and G. Bertrand, *J. Am. Chem. Soc.*, 1988, **110**, 6463–6466.
- A. J. I. Arduengo, R. L. Harlow and M. Kline, *J. Am. Chem. Soc.*, 1991, **113**, 361–363.
- H.-W. Wanzlick and H.-J. Schönherr, *Angew. Chem. Int. Ed. Engl.*, 1968, **7**, 141–142.
- K. Öfele, *J. Organomet. Chem.*, 1968, **12**, P42–P43.
- W. A. Herrmann, M. Elison, J. Fischer, C. Köcher and G. R. J. Artus, *Angew. Chem. Int. Ed. Engl.*, 1995, **34**, 2371–2374.
- J. Huang, G. Grasa and S. P. Nolan, *Org. Lett.*, 1999, **1**, 1307–1309.
- J. Huang and S. P. Nolan, *J. Am. Chem. Soc.*, 1999, **121**, 9889–9890.
- A. J. Arduengo III, United States, *US Pat.*, 5077414, 1991.
- X. Bantreil and S. P. Nolan, *Nat. Protoc.*, 2011, **6**, 69–77.
- C. Lorber and L. Vendier, *Dalton Trans.*, 2009, 6972–6984.
- C. Romain, S. Bellemin-Laponnaz and S. Dagorne, *Coord. Chem. Rev.*, 2020, **422**, 213411.
- L. Cerquera-Montealegre, D. Gallego and E. A. Baquero, in *Advances in Organometallic Chemistry*, Elsevier, 2024, vol. 81, pp. 181–270.
- A. A. Danopoulos, T. Simler and P. Braunstein, *Chem. Rev.*, 2019, **119**, 3730–3961.
- L. Jafarpour, J. Huang, E. D. Stevens and S. P. Nolan, *Organometallics*, 1999, **18**, 3760–3763.
- J. Huang, E. D. Stevens, S. P. Nolan and J. L. Petersen, *J. Am. Chem. Soc.*, 1999, **121**, 2674–2678.
- M. Scholl, T. M. Trnka, J. P. Morgan and R. H. Grubbs, *Tetrahedron Lett.*, 1999, **40**, 2247–2250.
- L. Ackermann, A. Fürstner, T. Weskamp, F. J. Kohl and W. A. Herrmann, *Tetrahedron Lett.*, 1999, **40**, 4787–4790.
- L. Jafarpour, H.-J. Schanz, E. D. Stevens and S. P. Nolan, *Organometallics*, 1999, **18**, 5416–5419.
- A. Fürstner, L. Ackermann, B. Gabor, R. Goddard, C. W. Lehmann, R. Mynott, F. Stelzer and O. R. Thiel, *Chem.-Eur. J.*, 2001, **7**, 3236–3253.
- L. Jafarpour, E. D. Stevens and S. P. Nolan, *J. Organomet. Chem.*, 2000, **606**, 49–54.
- A. C. Hillier, W. J. Sommer, B. S. Yong, J. L. Petersen, L. Cavallo and S. P. Nolan, *Organometallics*, 2003, **22**, 4322–4326.
- V. L. Chantler, S. L. Chatwin, R. F. R. Jazza, M. F. Mahon, O. Saker and M. K. Whittlesey, *Dalton Trans.*, 2008, 2603–2614.
- V. H. Mai and G. I. Nikonov, *Organometallics*, 2016, **35**, 943–949.
- M. K. Karunananda and N. P. Mankad, *Organometallics*, 2017, **36**, 220–227.
- J. Bosson and S. P. Nolan, *J. Org. Chem.*, 2010, **75**, 2039–2043.
- P. Nun, G. C. Fortman, A. M. Z. Slawin and S. P. Nolan, *Organometallics*, 2011, **30**, 6347–6350.
- S. P. Reade, M. F. Mahon and M. K. Whittlesey, *J. Am. Chem. Soc.*, 2009, **131**, 1847–1861.
- D. McKay, I. M. Riddlestone, S. A. Macgregor, M. F. Mahon and M. K. Whittlesey, *ACS Catal.*, 2015, **5**, 776–787.
- V. P. W. Böhm, C. W. K. Gstöttmayr, T. Weskamp and W. A. Herrmann, *Angew. Chem., Int. Ed.*, 2001, **40**, 3387–3389.
- B. Gradel, E. Brenner, R. Schneider and Y. Fort, *Tetrahedron Lett.*, 2001, **42**, 5689–5692.
- J. Louie, J. E. Gibby, M. V. Farnworth and T. N. Tekavec, *J. Am. Chem. Soc.*, 2002, **124**, 15188–15189.
- B. R. Dible and M. S. Sigman, *J. Am. Chem. Soc.*, 2003, **125**, 872–873.
- C. A. Tolman, *Chem. Rev.*, 1977, **77**, 313–348.
- R. Dorta, E. D. Stevens, N. M. Scott, C. Costabile, L. Cavallo, C. D. Hoff and S. P. Nolan, *J. Am. Chem. Soc.*, 2005, **127**, 2485–2495.
- R. A. Kelly III, H. Clavier, S. Giudice, N. M. Scott, E. D. Stevens, J. Bordner, I. Samardjiev, C. D. Hoff, L. Cavallo and S. P. Nolan, *Organometallics*, 2008, **27**, 202–210.
- D. G. Gusev, *Organometallics*, 2009, **28**, 6458–6461.
- S. Díez-González and S. P. Nolan, *Coord. Chem. Rev.*, 2007, **251**, 874–883.
- D. J. Nelson and S. P. Nolan, *Chem. Soc. Rev.*, 2013, **42**, 6723–6753.
- F. Vermersch, L. Oliveira, J. Hunter, M. Soleilhavoup, R. Jazza and G. Bertrand, *J. Org. Chem.*, 2022, **87**, 3511–3518.
- M. J. Iglesias, A. Prieto and M. C. Nicasio, *Org. Lett.*, 2012, **14**, 4318–4321.
- K. Matsubara, H. Yamamoto, S. Miyazaki, T. Inatomi, K. Nonaka, Y. Koga, Y. Yamada, L. F. Veiros and K. Kirchner, *Organometallics*, 2017, **36**, 255–265.
- V. Ritleng, A. M. Oertel and M. J. Chetcuti, *Dalton Trans.*, 2010, **39**, 8153–8160.



50 J. Buchspies, M. M. Rahman and M. Szostak, *Catalysts*, 2020, **10**, 372.

51 S. Kuhl, Y. Fort and R. Schneider, *J. Organomet. Chem.*, 2005, **690**, 6169–6177.

52 M. J. Iglesias, A. Prieto and M. C. Nicasio, *Adv. Synth. Catal.*, 2010, **352**, 1949–1954.

53 M. J. Iglesias, J. F. Blandez, M. R. Fructos, A. Prieto, E. Álvarez, T. R. Belderrain and M. C. Nicasio, *Organometallics*, 2012, **31**, 6312–6316.

54 S. G. Rull, J. F. Blandez, M. R. Fructos, T. R. Belderrain and M. C. Nicasio, *Adv. Synth. Catal.*, 2015, **357**, 907–911.

55 S. Nagao, T. Matsumoto, Y. Koga and K. Matsubara, *Chem. Lett.*, 2011, **40**, 1036–1038.

56 T. Inatomi, Y. Fukahori, Y. Yamada, R. Ishikawa, S. Kanegawa, Y. Koga and K. Matsubara, *Catal. Sci. Technol.*, 2019, **9**, 1784–1793.

57 J. S. Bair, Y. Schramm, A. G. Sergeev, E. Clot, O. Eisenstein and J. F. Hartwig, *J. Am. Chem. Soc.*, 2014, **136**, 13098–13101.

58 K. Matsubara, K. Ueno, Y. Koga and K. Hara, *J. Org. Chem.*, 2007, **72**, 5069–5076.

59 M. Henrion, M. J. Chetcuti and V. Ritleng, *Chem. Commun.*, 2014, **50**, 4624–4627.

60 J. A. Fernández-Salas, E. Marelli, D. B. Cordes, A. M. Z. Slawin and S. P. Nolan, *Chem.-Eur. J.*, 2015, **21**, 3906–3909.

61 Y. Schramm, M. Takeuchi, K. Semba, Y. Nakao and J. F. Hartwig, *J. Am. Chem. Soc.*, 2015, **137**, 12215–12218.

62 J. Diesel, A. M. Finogenova and N. Cramer, *J. Am. Chem. Soc.*, 2018, **140**, 4489–4493.

63 N. I. Saper, A. Ohgi, D. W. Small, K. Semba, Y. Nakao and J. F. Hartwig, *Nat. Chem.*, 2020, **12**, 276–283.

64 M. R. Chaulagain, G. M. Mahandru and J. Montgomery, *Tetrahedron*, 2006, **62**, 7560–7566.

65 Z. D. Miller, W. Li, T. R. Belderrain and J. Montgomery, *J. Am. Chem. Soc.*, 2013, **135**, 15282–15285.

66 S. Tamba, K. Shono, A. Sugie and A. Mori, *J. Am. Chem. Soc.*, 2011, **133**, 9700–9703.

67 S. Z. Tasker and T. F. Jamison, *J. Am. Chem. Soc.*, 2015, **137**, 9531–9534.

68 A. Kapat, T. Sperger, S. Guven and F. Schoenebeck, *Science*, 2019, **363**, 391–396.

69 M. Mendel, T. M. Karl, J. Hamm, S. J. Kaldas, T. Sperger, B. Mondal and F. Schoenebeck, *Nature*, 2024, **631**, 80–86.

70 A. J. Arduengo, H. V. R. Dias, J. C. Calabrese and F. Davidson, *Organometallics*, 1993, **12**, 3405–3409.

71 V. Jurkauskas, J. P. Sadighi and S. L. Buchwald, *Org. Lett.*, 2003, **5**, 2417–2420.

72 N. P. Mankad, D. S. Laitar and J. P. Sadighi, *Organometallics*, 2004, **23**, 3369–3371.

73 H. Kaur, F. K. Zinn, E. D. Stevens and S. P. Nolan, *Organometallics*, 2004, **23**, 1157–1160.

74 S. Díez-González, N. M. Scott and S. P. Nolan, *Organometallics*, 2006, **25**, 2355–2358.

75 S. Díez-González, E. D. Stevens, N. M. Scott, J. L. Petersen and S. P. Nolan, *Chem.-Eur. J.*, 2008, **14**, 158–168.

76 N. P. Mankad, T. G. Gray, D. S. Laitar and J. P. Sadighi, *Organometallics*, 2004, **23**, 1191–1193.

77 D. S. Laitar, E. Y. Tsui and J. P. Sadighi, *J. Am. Chem. Soc.*, 2006, **128**, 11036–11037.

78 T. Ohishi, M. Nishiura and Z. Hou, *Angew. Chem., Int. Ed.*, 2008, **47**, 5792–5795.

79 L. Zhang, J. Cheng and Z. Hou, *Chem. Commun.*, 2013, **49**, 4782–4784.

80 L. A. Goj, E. D. Blue, C. Munro-Leighton, T. B. Gunnoe and J. L. Petersen, *Inorg. Chem.*, 2005, **44**, 8647–8649.

81 L. A. Goj, E. D. Blue, S. A. Delp, T. B. Gunnoe, T. R. Cundari, A. W. Pierpont, J. L. Petersen and P. D. Boyle, *Inorg. Chem.*, 2006, **45**, 9032–9045.

82 C. Munro-Leighton, E. D. Blue and T. B. Gunnoe, *J. Am. Chem. Soc.*, 2006, **128**, 1446–1447.

83 S. A. Delp, C. Munro-Leighton, L. A. Goj, M. A. Ramírez, T. B. Gunnoe, J. L. Petersen and P. D. Boyle, *Inorg. Chem.*, 2007, **46**, 2365–2367.

84 G. C. Fortman, A. M. Z. Slawin and S. P. Nolan, *Organometallics*, 2010, **29**, 3966–3972.

85 I. I. F. Boogaerts, G. C. Fortman, M. R. L. Furst, C. S. J. Cazin and S. P. Nolan, *Angew. Chem., Int. Ed.*, 2010, **49**, 8674–8677.

86 L.-J. Cheng and N. P. Mankad, *J. Am. Chem. Soc.*, 2017, **139**, 10200–10203.

87 L.-J. Cheng, S. M. Islam and N. P. Mankad, *J. Am. Chem. Soc.*, 2018, **140**, 1159–1164.

88 D. R. Pye, L.-J. Cheng and N. P. Mankad, *Chem. Sci.*, 2017, **8**, 4750–4755.

89 L.-J. Cheng and N. P. Mankad, *J. Am. Chem. Soc.*, 2020, **142**, 80–84.

90 R. Sakae, K. Hirano and M. Miura, *J. Am. Chem. Soc.*, 2015, **137**, 6460–6463.

91 S. R. Sardini and M. K. Brown, *J. Am. Chem. Soc.*, 2017, **139**, 9823–9826.

92 J. Rae, K. Yeung, J. J. W. McDouall and D. J. Procter, *Angew. Chem., Int. Ed.*, 2016, **55**, 1102–1107.

93 K. Yeung, F. J. T. Talbot, G. P. Howell, A. P. Pulis and D. J. Procter, *ACS Catal.*, 2019, **9**, 1655–1661.

94 J. R. Bour, S. K. Kariofillis and M. S. Sanford, *Organometallics*, 2017, **36**, 1220–1223.

95 H. Sakaguchi, M. Ohashi and S. Ogoshi, *Angew. Chem., Int. Ed.*, 2018, **57**, 328–332.

96 J. Li, L. Wang, Z. Zhao, X. Li, X. Yu, P. Huo, Q. Jin, Z. Liu, Z. Bian and C. Huang, *Angew. Chem., Int. Ed.*, 2020, **59**, 8210–8217.

97 P. de Frémont, N. M. Scott, E. D. Stevens and S. P. Nolan, *Organometallics*, 2005, **24**, 2411–2418.

98 E. A. Martynova, N. V. Tzouras, G. Pisano, C. S. J. Cazin and S. P. Nolan, *Chem. Commun.*, 2021, **57**, 3836–3856.

99 M. R. Fructos, T. R. Belderrain, P. de Frémont, N. M. Scott, S. P. Nolan, M. M. Díaz-Requejo and P. J. Pérez, *Angew. Chem., Int. Ed.*, 2005, **44**, 5284–5288.

100 M. R. Fructos, P. de Frémont, S. P. Nolan, M. M. Díaz-Requejo and P. J. Pérez, *Organometallics*, 2006, **25**, 2237–2241.

101 C. F. Bender and R. A. Widenhoefer, *Org. Lett.*, 2006, **8**, 5303–5305.

102 C. A. Witham, P. Mauleón, N. D. Shapiro, B. D. Sherry and F. D. Toste, *J. Am. Chem. Soc.*, 2007, **129**, 5838–5839.



103 G. Li and L. Zhang, *Angew. Chem., Int. Ed.*, 2007, **46**, 5156–5159.

104 P. de Frémont, E. D. Stevens, M. R. Fructos, M. M. Díaz-Requejo, P. J. Pérez and S. P. Nolan, *Chem. Commun.*, 2006, 2045–2047.

105 N. Marion, S. Díez-González, P. de Frémont, A. R. Noble and S. P. Nolan, *Angew. Chem., Int. Ed.*, 2006, **45**, 3647–3650.

106 P. Nun, S. Gaillard, A. Poater, L. Cavallo and S. P. Nolan, *Org. Biomol. Chem.*, 2010, **9**, 101–104.

107 L. Ricard and F. Gagosc, *Organometallics*, 2007, **26**, 4704–4707.

108 M. Jia and M. Bandini, *ACS Catal.*, 2015, **5**, 1638–1652.

109 D. Zuccaccia, A. Del Zotto and W. Baratta, *Coord. Chem. Rev.*, 2019, **396**, 103–116.

110 Z. Lu, G. B. Hammond and B. Xu, *Acc. Chem. Res.*, 2019, **52**, 1275–1288.

111 C. H. M. Amijs, V. López-Carrillo, M. Raducan, P. Pérez-Galán, C. Ferrer and A. M. Echavarren, *J. Org. Chem.*, 2008, **73**, 7721–7730.

112 A. S. K. Hashmi, A. M. Schuster and F. Rominger, *Angew. Chem., Int. Ed.*, 2009, **48**, 8247–8249.

113 N. Marion, R. S. Ramón and S. P. Nolan, *J. Am. Chem. Soc.*, 2009, **131**, 448–449.

114 S. Gaillard, A. M. Z. Slawin and S. P. Nolan, *Chem. Commun.*, 2010, **46**, 2742–2744.

115 S. Gaillard, J. Bosson, R. S. Ramón, P. Nun, A. M. Z. Slawin and S. P. Nolan, *Chem.-Eur. J.*, 2010, **16**, 13729–13740.

116 D. Wang, R. Cai, S. Sharma, J. Jirak, S. K. Thummanapelli, N. G. Akhmedov, H. Zhang, X. Liu, J. L. Petersen and X. Shi, *J. Am. Chem. Soc.*, 2012, **134**, 9012–9019.

117 I. I. F. Boogaerts and S. P. Nolan, *J. Am. Chem. Soc.*, 2010, **132**, 8858–8859.

118 R. S. Ramón, S. Gaillard, A. Poater, L. Cavallo, A. M. Z. Slawin and S. P. Nolan, *Chem.-Eur. J.*, 2011, **17**, 1238–1246.

119 Y. Oonishi, A. Gómez-Suárez, A. R. Martin and S. P. Nolan, *Angew. Chem., Int. Ed.*, 2013, **52**, 9767–9771.

120 A. Gómez-Suárez, Y. Oonishi, A. R. Martin, S. V. C. Vummaleti, D. J. Nelson, D. B. Cordes, A. M. Z. Slawin, L. Cavallo, S. P. Nolan and A. Poater, *Chem.-Eur. J.*, 2016, **22**, 1125–1132.

121 I. Braun, A. M. Asiri and A. S. K. Hashmi, *ACS Catal.*, 2013, **3**, 1902–1907.

122 R. M. P. Veenboer, S. Dupuy and S. P. Nolan, *ACS Catal.*, 2015, **5**, 1330–1334.

123 S. Dupuy, D. Gasperini and S. P. Nolan, *ACS Catal.*, 2015, **5**, 6918–6921.

124 A. S. K. Hashmi, I. Braun, M. Rudolph and F. Rominger, *Organometallics*, 2012, **31**, 644–661.

125 A. S. K. Hashmi, M. Wieteck, I. Braun, P. Nösel, L. Jongbloed, M. Rudolph and F. Rominger, *Adv. Synth. Catal.*, 2012, **354**, 555–562.

126 A. S. K. Hashmi, T. Lauterbach, P. Nösel, M. H. Vilhelmsen, M. Rudolph and F. Rominger, *Chem.-Eur. J.*, 2013, **19**, 1058–1065.

127 S. Ferrer and A. M. Echavarren, *Organometallics*, 2018, **37**, 781–786.

128 Y. He, Z. Li, K. Robeyns, L. Van Meervelt and E. V. Van der Eycken, *Angew. Chem., Int. Ed.*, 2018, **57**, 272–276.

129 Z. Li, L. Song, L. Van Meervelt, G. Tian and E. V. Van der Eycken, *ACS Catal.*, 2018, **8**, 6388–6393.

130 Y.-B. Bai, Z. Luo, Y. Wang, J.-M. Gao and L. Zhang, *J. Am. Chem. Soc.*, 2018, **140**, 5860–5865.

131 P. D. Jadhav, X. Lu and R.-S. Liu, *ACS Catal.*, 2018, **8**, 9697–9701.

132 R. Gauthier, N. V. Tzouras, Z. Zhang, S. Bédard, M. Saab, L. Falivene, K. Van Hecke, L. Cavallo, S. P. Nolan and J.-F. Paquin, *Chem.-Eur. J.*, 2022, **28**, e202103886.

133 M. Gatto, A. Del Zotto, J. Segato and D. Zuccaccia, *Organometallics*, 2018, **37**, 4685–4691.

134 M. Jin, R. Ando, M. J. Jellen, M. A. Garcia-Garibay and H. Ito, *J. Am. Chem. Soc.*, 2021, **143**, 1144–1153.

135 E. A. Martynova, V. A. Voloshkin, S. G. Guillet, F. Bru, M. Beliš, K. V. Hecke, C. S. J. Cazin and S. P. Nolan, *Chem. Sci.*, 2022, **13**, 6852–6857.

136 V. A. Voloshkin, M. Villa, E. A. Martynova, M. Beliš, K. V. Hecke, P. Ceroni and S. P. Nolan, *Chem. Sci.*, 2024, **15**, 4571–4580.

137 H. M. Lee and S. P. Nolan, *Org. Lett.*, 2000, **2**, 2053–2055.

138 G. A. Grasa and S. P. Nolan, *Org. Lett.*, 2001, **3**, 119–122.

139 M. S. Viciu, R. M. Kissling, E. D. Stevens and S. P. Nolan, *Org. Lett.*, 2002, **4**, 2229–2231.

140 M. S. Viciu, R. F. Germaneau and S. P. Nolan, *Org. Lett.*, 2002, **4**, 4053–4056.

141 O. Diebolt, P. Braunstein, S. P. Nolan and C. S. J. Cazin, *Chem. Commun.*, 2008, 3190–3192.

142 S. Yang, T. Zhou, A. Poater, L. Cavallo, S. P. Nolan and M. Szostak, *Catal. Sci. Technol.*, 2021, **11**, 3189–3197.

143 T. Zhou, S. Ma, F. Nahra, A. M. C. Obled, A. Poater, L. Cavallo, C. S. J. Cazin, S. P. Nolan and M. Szostak, *iScience*, 2020, **23**, 101377.

144 M. S. Viciu, R. F. Germaneau, O. Navarro-Fernandez, E. D. Stevens and S. P. Nolan, *Organometallics*, 2002, **21**, 5470–5472.

145 G. M. Meconi, S. V. C. Vummaleti, J. A. Luque-Urrutia, P. Belanzoni, S. P. Nolan, H. Jacobsen, L. Cavallo, M. Solà and A. Poater, *Organometallics*, 2017, **36**, 2088–2095.

146 O. Navarro, H. Kaur, P. Mahjoor and S. P. Nolan, *J. Org. Chem.*, 2004, **69**, 3173–3180.

147 O. Navarro, R. A. Kelly and S. P. Nolan, *J. Am. Chem. Soc.*, 2003, **125**, 16194–16195.

148 M. S. Viciu, R. A. Kelly, E. D. Stevens, F. Naud, M. Studer and S. P. Nolan, *Org. Lett.*, 2003, **5**, 1479–1482.

149 O. Navarro, N. Marion, Y. Oonishi, R. A. Kelly and S. P. Nolan, *J. Org. Chem.*, 2006, **71**, 685–692.

150 Z. Lian, B. N. Bhawal, P. Yu and B. Morandi, *Science*, 2017, **356**, 1059–1063.

151 D. R. Jensen and M. S. Sigman, *Org. Lett.*, 2003, **5**, 63–65.

152 D. R. Jensen, M. J. Schultz, J. A. Mueller and M. S. Sigman, *Angew. Chem., Int. Ed.*, 2003, **42**, 3810–3813.

153 J. A. Mueller, C. P. Goller and M. S. Sigman, *J. Am. Chem. Soc.*, 2004, **126**, 9724–9734.

154 M. J. Schultz, S. S. Hamilton, D. R. Jensen and M. S. Sigman, *J. Org. Chem.*, 2005, **70**, 3343–3352.



155 C. N. Cornell and M. S. Sigman, *J. Am. Chem. Soc.*, 2005, **127**, 2796–2797.

156 E. W. Werner, K. B. Urkalan and M. S. Sigman, *Org. Lett.*, 2010, **12**, 2848–2851.

157 E. W. Werner and M. S. Sigman, *J. Am. Chem. Soc.*, 2010, **132**, 13981–13983.

158 C. J. O'Brien, E. A. B. Kantchev, C. Valente, N. Hadei, G. A. Chass, A. Lough, A. C. Hopkinson and M. G. Organ, *Chem.-Eur. J.*, 2006, **12**, 4743–4748.

159 S. G. Guillet, V. A. Voloshkin, M. Saab, M. Beliš, K. V. Hecke, F. Nahra and S. P. Nolan, *Chem. Commun.*, 2020, **56**, 5953–5956.

160 M. G. Organ, M. Abdel-Hadi, S. Avola, I. Dubovyk, N. Hadei, E. A. B. Kantchev, C. J. O'Brien, M. Sayah and C. Valente, *Chem.-Eur. J.*, 2008, **14**, 2443–2452.

161 M. G. Organ, S. Avola, I. Dubovyk, N. Hadei, E. A. B. Kantchev, C. J. O'Brien and C. Valente, *Chem.-Eur. J.*, 2006, **12**, 4749–4755.

162 M. G. Organ, M. Abdel-Hadi, S. Avola, N. Hadei, J. Nasielski, C. J. O'Brien and C. Valente, *Chem.-Eur. J.*, 2007, **13**, 150–157.

163 E. D. Patil, J. V. Burykina, D. B. Eremin, D. A. Boiko, K. E. Shepelenko, V. V. Ilyushenkova, V. M. Chernyshev and V. P. Ananikov, *Inorg. Chem.*, 2024, **63**, 2967–2976.

164 V. M. Chernyshev, E. A. Denisova, D. B. Eremin and V. P. Ananikov, *Chem. Sci.*, 2020, **11**, 6957–6977.

165 N. Marion, O. Navarro, J. Mei, E. D. Stevens, N. M. Scott and S. P. Nolan, *J. Am. Chem. Soc.*, 2006, **128**, 4101–4111.

166 C. C. Johansson Seechurn, S. L. Parisel and T. J. Colacot, *J. Org. Chem.*, 2011, **76**, 7918–7932.

167 T. Ben Halima, W. Zhang, I. Yalaoui, X. Hong, Y.-F. Yang, K. N. Houk and S. G. Newman, *J. Am. Chem. Soc.*, 2017, **139**, 1311–1318.

168 P. Lei, G. Meng and M. Szostak, *ACS Catal.*, 2017, **7**, 1960–1965.

169 F. Izquierdo, C. Zinser, Y. Minenkov, D. B. Cordes, A. M. Z. Slawin, L. Cavallo, F. Nahra, C. S. J. Cazin and S. P. Nolan, *ChemCatChem*, 2018, **10**, 601–611.

170 G. Meng, P. Lei and M. Szostak, *Org. Lett.*, 2017, **19**, 2158–2161.

171 G. Li, T. Zhou, A. Poater, L. Cavallo, S. P. Nolan and M. Szostak, *Catal. Sci. Technol.*, 2020, **10**, 710–716.

172 N. Marion, E. C. Eearnot, O. Navarro, D. Amoroso, A. Bell and S. P. Nolan, *J. Org. Chem.*, 2006, **71**, 3816–3821.

173 P. R. Melvin, A. Nova, D. Balcells, W. Dai, N. Hazari, D. P. Hruszkewycz, H. P. Shah and M. T. Tudge, *ACS Catal.*, 2015, **5**, 3680–3688.

174 F. Nahra, D. J. Nelson and S. P. Nolan, *Trends Chem.*, 2020, **2**, 1096–1113.

175 A. J. Arduengo, R. Krafczyk, R. Schmutzler, H. A. Craig, J. R. Goerlich, W. J. Marshall and M. Unverzagt, *Tetrahedron*, 1999, **55**, 14523–14534.

176 M. B. Dinger and J. C. Mol, *Adv. Synth. Catal.*, 2002, **344**, 671–677.

177 F. C. Courchay, J. C. Sworen and K. B. Wagener, *Macromolecules*, 2003, **36**, 8231–8239.

178 N. Marion, O. Navarro, J. Mei, E. D. Stevens, N. M. Scott and S. P. Nolan, *J. Am. Chem. Soc.*, 2006, **128**, 4101–4111.

179 J. A. Akana, K. X. Bhattacharyya, P. Müller and J. P. Sadighi, *J. Am. Chem. Soc.*, 2007, **129**, 7736–7737.

180 B. T. Worrell, J. A. Malik and V. V. Fokin, *Science*, 2013, **340**, 457–460.

181 M. G. Organ, S. Çalimsiz, M. Sayah, K. H. Hoi and A. J. Lough, *Angew. Chem., Int. Ed.*, 2009, **48**, 2383–2387.

182 S. Meiries, G. Le Duc, A. Chartoire, A. Collado, K. Speck, K. S. A. Arachchige, A. M. Z. Slawin and S. P. Nolan, *Chem.-Eur. J.*, 2013, **19**, 17358–17368.

183 S. Sharif, R. P. Rucker, N. Chandrasoma, D. Mitchell, M. J. Rodriguez, R. D. J. Froese and M. G. Organ, *Angew. Chem., Int. Ed.*, 2015, **54**, 9507–9511.

184 B. Atwater, N. Chandrasoma, D. Mitchell, M. J. Rodriguez, M. Pompeo, R. D. J. Froese and M. G. Organ, *Angew. Chem., Int. Ed.*, 2015, **54**, 9502–9506.

185 G. Berthon-Gelloz, M. A. Siegler, A. L. Spek, B. Tinant, J. N. H. Reek and I. E. Markó, *Dalton Trans.*, 2010, **39**, 1444–1446.

186 Y. Makida, E. Marelli, A. M. Z. Slawin and S. P. Nolan, *Chem. Commun.*, 2014, **50**, 8010–8013.

187 M. Delarmelina, E. Marelli, J. W. d. M. Carneiro, S. P. Nolan and M. Bühl, *Chem.-Eur. J.*, 2017, **23**, 14954–14961.

188 A. R. Martin, Y. Makida, S. Meiries, A. M. Z. Slawin and S. P. Nolan, *Organometallics*, 2013, **32**, 6265–6270.

189 A. Chartoire, M. Lesieur, L. Falivene, A. M. Z. Slawin, L. Cavallo, C. S. J. Cazin and S. P. Nolan, *Chem.-Eur. J.*, 2012, **18**, 4517–4521.

190 A. Chartoire, X. Frogneux and S. P. Nolan, *Adv. Synth. Catal.*, 2012, **354**, 1897–1901.

191 Q. Shen, T. Ogata and J. F. Hartwig, *J. Am. Chem. Soc.*, 2008, **130**, 6586–6596.

192 A. Chartoire, A. Boreux, A. R. Martin and S. P. Nolan, *RSC Adv.*, 2013, **3**, 3840–3843.

193 F. Izquierdo, A. Chartoire and S. P. Nolan, *ACS Catal.*, 2013, **3**, 2190–2193.

194 S. G. Weber, C. Loos, F. Rominger and B. F. Straub, *Arkivoc*, 2012, **2012**, 226–242.

195 S. G. Weber, D. Zahner, F. Rominger and B. F. Straub, *Chem. Commun.*, 2012, **48**, 11325–11327.

196 S. G. Weber, F. Rominger and B. F. Straub, *Eur. J. Inorg. Chem.*, 2012, **2012**, 2863–2867.

197 S. G. Weber, D. Zahner, F. Rominger and B. F. Straub, *ChemCatChem*, 2013, **5**, 2330–2335.

198 Q. Zhao, G. Meng, G. Li, C. Flach, R. Mendelsohn, R. Lalancette, R. Szostak and M. Szostak, *Chem. Sci.*, 2021, **12**, 10583–10589.

199 G. Utecht-Jarzyńska, S. Jarzyński, M. M. Rahman, G. Meng, R. Lalancette, R. Szostak and M. Szostak, *Organometallics*, 2024, **43**, 2305–2313.

200 R. Manne, S. Sharma, S. Dey, S. K. Patil, N. Nehra, H. Rawool, G. Rajaraman and P. Ghosh, *J. Mol. Struct.*, 2024, **1316**, 139022.

